Sub 500 nm refractory carbonaceous particles in the polar stratosphere

Katharina Schütze[1,3], James C. Wilson[2], Stephan Weinbruch[1], Nathalie Benker[1], Martin Ebert[1], Ralf Weigel[3], Stephan Borrmann[3,4]

[1]Institut für Angewandte Geowissenschaften, Technische Universität Darmstadt, Darmstadt, Germany
[2]Department of Mechanical and Materials Engineering, University of Denver, Denver, CO 80208, USA
[3]Institut für Physik der Atmosphäre, Johannes Gutenberg-Universität, Mainz, Germany
[4]Partikelchemie, Max-Planck-Institut für Chemie, Mainz, Germany

Correspondence to: Katharina Schütze (schuetze@geo.tu-darmstadt.de)

Abstract. Eleven particle samples collected in the polar stratosphere during SOLVE (SAGE III Ozone loss and validation experiment) from January until March 2000 were characterized in detail by high-resolution transmission and scanning electron microscopy (TEM/SEM) combined with energy-dispersive X-ray microanalysis. A total number of 4175 particles (TEM=3845; SEM=330) was analyzed from these samples which were collected mostly inside the polar vortex in the altitude range between 17.3 and 19.9 km. By particle volume, all samples are dominated by volatile particles (ammonium sulfates/hydrogen sulfates). By number, approximately 28 – 82 % of the particles are refractory carbonaceous with sizes between 20 - 830 nm. Internal mixtures of refractory carbonaceous and volatile particles comprise up to 16 %, individual volatile particles about 9 to 72 %.

Most of the refractory carbonaceous particles are completely amorphous, a few of the particles are partly ordered with a graphene sheet separation distance of 0.37 ± 0.06 nm (mean value ± standard deviation). Carbon and oxygen are the only detected major elements with an atomic O/C ratio of 0.11 ± 0.07. Minor elements observed include Si, S, Fe, Cr and Ni with the following atomic ratios relative to C: Si/C: 0.010 ± 0.011; S/C: 0.0007 ± 0.0015; Fe/C: 0.0052 ± 0.0074; Cr/C: 0.0012 ± 0.0017; Ni/C: 0.0006 ± 0.0011 (all mean values ± standard deviation).

High resolution element distribution images reveal that the minor elements are distributed within the carbonaceous matrix, i.e., heterogeneous inclusions are not observed. No difference in size, nanostructure and elemental composition was found between particles collected inside and outside the polar vortex.

Based on chemistry and nanostructure, aircraft exhaust, volcanic emissions and biomass burning can certainly be excluded as source. The same is true for the less probable, but globally important sources: wood burning, coal burning, diesel engines and ship emissions.

Rocket exhaust and carbonaceous material from interplanetary dust particles remain as possible sources of the refractory carbonaceous particles studied. However, additional work is required in order to identify the sources unequivocally.

1 Introduction

The chemistry of stratospheric aerosols has been studied for more than half a century (Junge et al., 1961; Junge 1963), and it was discovered that sulfur is the main particle component. Junge and Manson (1961) supposed the particles to consist of ammonium sulfate, and Bigg et al. (1970) suggested sulfuric acid with varying amounts of ammonia. Rosen et al. (1971)

5   strengthened the evidence for the material to be sulfuric acid as most of the material evaporated at the temperature expected for this substance. According to Bigg (1975), the majority of the particles is composed of sulfuric acid with varying amounts of ammonium sulfate.

In addition to the dominating sulfur-rich particles (sulfuric acid, sulfates), refractory particles were reported frequently. Dense,

10 mineral-rich particles presumably originating from the eruption of the Mt. Agung volcano were observed by Mossop (1963, 1965) using scanning electron microscopy. However, due to the lack of instrumentation, the chemistry of the particles could not be investigated. Refractory particles with diameters >1 µm were studied in more detail by Zolensky and Mackinnon (1985), and several groups were distinguished: chondrite, silicate, aluminum (Al), aluminum with variable amounts of other elements, iron (Fe) with or without sulfate (S), calcium (Ca)-Al silicates and "other" particles. The silicate particles were dominant and

15 interpreted to be volcanic, probably from the Mt. St. Helens eruption in 1980. In contrast to prior findings, a large refractory stratospheric particle load was recognized by Zolensky et al. (1989). He assumed that this increase was caused by solid rocket exhaust or the re-entry of debris associated to human space flight activity (inoperative satellites, burnt out rocket stages, tools, etc.). According to Sheridan et al. (1994) approximately 97% of all analyzed stratospheric particles were sulfuric acid. Also non-sulfate materials, soot, other C-rich substances and crustal material were detected. Carbonaceous aerosol was found to be

20 widely distributed in the lower and middle stratosphere and interplanetary dust was significantly abundant above 30 km (Renard et al., 2008). Della Corte et al., 2013 found calcium-oxygen (CaO) -rich particles probably originating from a bolide that penetrated the earth' atmosphere. Single particle mass spectrometry (SPMS) brought new insights into the chemistry of stratospheric particles (e.g., Murphy et al., 1998, 2007, 2013). According to these authors, stratospheric particles are dominated by pure sulfuric acid, sulfuric acid internally mixed with material from ablated meteoroids, and mixtures of organic-sulfate

25 particles. A recent SEM study by Ebert et al. (2016) focused on refractory particles in the late winter stratospheric polar vortex. The main particle groups encountered included Fe-rich, Si-rich, Ca-rich, metal mixtures and Carbon (C)/Si-rich particles.

Refractory particles in the UT/LS (Upper Troposphere / Lower Stratosphere) can act as condensation nuclei for cirrus clouds (Kojima et al., 2004; 2005; Cziczo et al., 2013) and as surfaces for heterogeneous chemical reactions in the polar stratosphere

30 which play a significant role in polar ozone depletion (e.g., Peter, 1997; Solomon, 1999; Peter and Grooß, 2012). In addition, the particles can serve as surfaces for the heterogeneous condensation of saturated gases in the polar stratosphere (Saunders et al. 2010, 2012; Bigg, 2012; Frankland et al., 2015, Voigt et al. 2005; Hoyle et al. 2013; Engel et al. 2013). Due to the acidic environment, the particles can (partially) dissolve in the acidic solution droplets (binary HNO_3-H_2O or ternary HNO_3-H_2SO_4-

H_2O) and, thus, change their freezing properties. Therefore, the dissolved particles in a ternary HNO_3-H_2SO_4-H_2O solution could have an important impact on the formation of polar stratospheric clouds (PSCs). As gaseous compounds will condense on refractory particles, they will grow, both in size and mass, which leads to a change in their sedimentation velocity (Fromm et al. 2000; Jost et al., 2004). Therefore, the gaseous compounds can either be redistributed in the stratospheric region or sediment out more quickly.

There are multiple sources which contribute to the stratospheric refractory particle load. Interplanetary dust particles are considered to be the major component of refractory material (Murphy et al., 1998; 2007; Plane, 2012). Another important source of stratospheric refractory particles are volcanic eruptions which may either eject material directly into the stratosphere (Vernier et al., 2011) or lead to particle transport through the tropical transition layer (TTL) (Mattis et al., 2010). Further potential sources of stratospheric refractory particles are high-flying aircraft (Fahey et al, 1995; Pueschel et al., 1997, Petzold et al., 1999), rockets (Newman et al., 2001), ablated material from meteorites (Hunten et al. 1980; Turco et al., 1981; Murphy et al., 1998; Cziczo et al., 2001) and all kinds of terrestrial material being lifted and entrained into the stratosphere by the Brewer-Dobson-Circulation (Holton et al., 1995, Austin and Li, 2006).

In summary, a variety of different refractory particle types is observed in the stratosphere. Due to the still limited number of sampling and measurement campaigns, the occurrence as well as the sources of refractory particles is not known precisely. The present paper first aims at improving the database on the observed particle groups. Second, it is attempted to infer potential sources by a detailed characterization using high-resolution transmission electron microscopy (TEM), scanning electron microscopy (SEM) and energy-dispersive X-ray microanalysis (EDX).

2 Experimental

2.1 Sampling

Stratospheric particles were sampled on board of the NASA ER-2 aircraft during the SAGE III Ozone loss and validation experiment (SOLVE), which was conducted in January-March 2000 in Kiruna (Sweden). The Multi-Sample Aerosol Collection System (MACS) (Kojima et al., 2004), a thin-plate low-pressure impactor was used for sampling. The particles were deposited on transmission electron microscopy (TEM) copper (Cu) grids covered with a formvar film. The MACS is designed to collect up to 23 samples, of which the first one always serves as a blank sample for reference. Sampling date, flight characteristics, potential vorticity (PV), maximum altitude, pressure and potential temperature are summarized for the analyzed grids in Table 1.

The meteorological conditions of the early winter (November – January) northern hemispheric polar vortex of 1999/2000 are described in detail by Manney and Sabutis, 2000. The early winter (November – January) northern hemispheric polar vortex of 1999/2000 had much lower averaged temperatures compared to any previously observed Arctic winter. It was weaker than

the early winter polar vortices of the previous years. The vortex was discontinuous in the middle of December, with a large extent in the upper and small extend in the lower stratosphere. By mid-January, the vortex evolved to be continuous and stable until mid-March (Greenblatt et al., 2002). Jost et al. (2002) describe anomalous single mixing events occurring during that time at the potential temperature (PT) range of 350-500 K. These events are probably the result of mixing between deep vortex

5 and extra vortex air.

The stratospheric particle samples (deposited on TEM grids) taken within the polar vortex, were packed into single plastic boxes and stored in a desiccator prior to analysis. In total, 122 samples from 15 sampling days were collected.

2.2 Electron microscopy

A total of 4175 particles (3845 TEM; 330 SEM) from 11 samples were investigated by transmission and scanning electron

10 microscopy. The samples were selected according to meteorological conditions and suitability for electron microscopy (i.e., substrate area covered by particles).

The scope of this study is the detailed characterization of refractory stratospheric particles. According to Ebert et al., 2016, we have classified all particles that are stable (no visible morphological change) under the high vacuum conditions and electron beam excitation in the SEM and TEM as refractory.

15 The size, morphology, mixing state, nanostructure and chemical composition of 60 refractory particles per sample were studied by TEM using a Philips CM20 instrument (FEI, Eindhoven, The Netherlands) operated at 200 kV electron accelerating voltage. The chemical composition of the particles (all elements with an atomic number Z ☐ 5) was determined by EDX using a Silicon-drift X-ray detector (Oxford Instruments, Oxfordshire, United Kingdom) and a measurement time of 20 seconds. Particle size and graphene sheet separation distance were analyzed by the ImageJ (1.48v; Rasband, W. S. National Institutes of Health,

20 USA, 1997-2016) software. Element distribution images were acquired with a JEOL JEM 2100F (JEOL, Tokyo, Japan) operated in Scanning Transmission Electron Microscopy (STEM) mode at an electron acceleration voltage of 200 kV. The instrument is equipped with an energy-dispersive X-ray Silicon-drift detector (Oxford, Wiesbaden, Germany).

In order to detect elements present at low abundance, additional 30 refractory particles per sample were analyzed by SEM using a Quanta 200 FEG instrument (FEI, Eindhoven, The Netherlands) equipped with an energy-dispersive X-ray detector

25 (EDAX, Tilburg, The Netherlands) operated at 15 kV electron accelerating voltage. X-ray spectra were accumulated over fifteen minutes per particle to obtain a low detection limit. These longtime-measurements were not possible in the TEM due to a much higher beam energy leading to particle evaporation, which prevents further particle analysis. Element concentrations were obtained from the X-ray count rates by applying a "standard-less" ZAF correction. Detection limits of element/carbon ratios (at% / at%) for the long-time measurements are as follows: O/C = 0.0034; Si/C = 0.0010; S/C = 0.0008; Cr/C = 0.0008;

30 Fe/C = 0.0009 and Ni/C = 0.0011.

The particles were studied by TEM and SEM without coating.

Potential contamination of the samples was checked by investigating blanks (samples transported in the MACS but not exposed to stratospheric air) for each sampling day. A few titanium (Ti) and zinc (Zn) oxide particles, as well as few pure C particles

were encountered on the blank samples. They look similar to some carbonaceous particles being described as contaminants on TEM grids (Harris et al., 2001). However, these particles are different in both size and morphology compared to the particles observed in the impaction spot of the samples.

In order to verify that the small amounts of Fe, chromium (Cr) and nickel (Ni) detected during long-term SEM measurements are not artifacts from the substrate, five points on each substrate far away from particles were analyzed. All three elements were not detected in these substrate measurements.

Another possible artifact that could impair the measurement of elements present at low concentration is scattered radiation within the SEM. To exclude this possibility, one sample was measured at different sample chamber pressures (5x10-3, 200 and 500 Pa). Under the elevated pressures significant scattering of beam electrons occurs in the sample chamber. According to Stokes (2008), the extent of scattering varies between 40 – 80 % at 200 Pa and 70 – 98 % at 500 Pa. However, even with this large extent of scattering the elements Fe, Cr, and Ni did not show elevated concentrations. In contrast, when increasing the pressure in the vacuum chamber (i.e., increasing scattering of beam electrons) the count rates of these elements decreased. Thus, it is concluded, that the low Fe, Cr and Ni concentrations detected in individual particles are real, i.e., they are not excited by stray radiation.

The chemical composition of the particles was determined by EDX in TEM (n = 529) as well as SEM (n = 330). Due to the small size of the particles, TEM is the method of first choice when analyzing the particles. As mentioned above, particles were additionally analyzed by SEM. Both measurements led to small but systematic differences in element ratios of O, Si, S, Mg (magnesium), Fe and Al relative to C (Figure S1 of the electronic supplement). For all elements TEM-EDX yielded somewhat higher elemental ratios (relative to carbon) than SEM-EDX. These differences are most likely the result of the different properties of the detectors (i.e., thickness of detector windows) and the highly different acceleration voltage (15 kV in SEM versus 200 kV in TEM). However, as the differences are small, our conclusions are independent of the method used. SEM-EDX data are used throughout the present paper, as the counting time on each particle was much longer in SEM (15 minutes) than in TEM (20 seconds) leading to higher precision as well as lower detection limits. The much lower detection limits of SEM-EDX are important for source identification as minor elements may serve as fingerprint for several anthropogenic and natural sources. Thus, the SEM-EDX data are preferred despite the lower number of particles investigated with this technique. In addition, the chemical composition of particles could not be analyzed by TEM-EDX on two samples (labeled as G and K) due to the inappropriate position of the impaction spot on the substrate (to close to the Cu grid leading to a very high count rate for Cu).

In order to assess the relative abundance of refractory particles per sample, additional image analysis was performed in TEM. For this purpose image series before and after TEM analysis were prepared. The destruction respectively morphological change after TEM analysis allows the assignment if individual particles were refractory, volatile or mixtures of both. All particles that are stable after electron beam treatment and not showing any change in morphology are classified as refractory. In contrast, volatile particles evaporate rapidly. In total 3316 particles were analyzed by this method.

To ensure unbiased results, the individual images as well as particles for EDX analysis were randomly taken in inner and outer areas of the impaction spot.

2.3 Statistical analysis

Censored boxplots show data taking into account the fraction of values below detection limit. Lower and upper quartiles appear as a box, minimum and maximum values as whiskers.

Differences in element ratios between samples collected inside and outside the vortex were tested with the generalized Wilcoxon test (Helsel, 2012) applying a significance-level of 5%. Differences in size, projected area diameter and element ratios between the various samples were tested with the Kruskal-Wallis rank sum test (uncensored data) and the generalized Wilcoxon test (censored data). In all individual tests, s significance level of 5 % was applied.

Detection limits were calculated from counting statistics (background counts plus three times standard deviation of background counts).

All statistical calculations were performed with R (version 3.3.0; R Core Team, 2016) and using the contributed package NADA (version 1.5-6; Lee, 2013).

3 Results

All particles are located within a characteristic impaction spot. As TEM bright field images show, (Figure 1) volatile particles (initially deposited as droplets) cover a relatively larger area compared to refractory particles. They show high abundances of sulfur and oxygen. Sometimes, a minor nitrogen peak is also observed in the X-ray spectra. These particles are highly unstable under electron bombardment. They most likely consist of ammonium sulfate/hydrogen sulfate and formed from sulfuric/nitric acid. As the presence of sulfates in stratospheric samples is well known (e.g., Sheridan et al., 1989, 1994; Arnold et al., 1998; Murphy et al., 2007; Kremser et al., 2016), these particles are not investigated further. In addition to the sulfates, carbonaceous particles stable under electron bombardment are frequently observed either as individual particles or embedded in the sulfates (Figures 1 and 2).

As the refractory carbonaceous particles in Figure 2a have no distinct shape and surface morphology, only one TEM image is shown.

By number, the refractory particles are dominating in all samples, except for sample G (Figure 3). In most of the samples, less than 10% of the particles are internal mixtures of refractory and volatile particles. Please note that each droplet – now consisting of mainly one large particle surrounded by many smaller ones – is counted as one particle.

TEM Analysis of the size distribution of the particles

The size distribution of the refractory carbonaceous particles is shown in Figure 4. Approximately 98 % of the particles have an equivalent projected area diameter (D_{pa}) below 500 nm (range 20 – 830 nm). The size of the particles slightly increases with time during the campaign, sample J shows the largest median particle sizes.

5 *SEM Analysis of the chemical composition of the refractory carbonaceous particles*

The refractory carbonaceous particles always contain besides C also O, Si, and S (Figures 2, 5 and 6). The elements Cr, Fe, and Ni are often found as minor component (Figure 5). As the TEM substrates are made of a formvar foil predominantly consisting of C, O, and traces of Si, these three elements may – at least partly – be an artifact of the substrate. There are three points of evidence which clearly show that the refractory carbonaceous particles observed are not an artifact of the substrate:

1) Much higher carbon X-ray count rates were obtained when measuring particles compared to the pure substrate.
2) Graphene sheets within the particles were observed by high resolution TEM. In contrast, the substrate is always completely amorphous.
3) The refractory carbonaceous particles only occur within the impaction spot.

The refractory carbonaceous particles have a different morphology than the few carbonaceous particles found on blank samples. In addition, the carbonaceous particles encountered on blank samples are often much larger with a size of several µm. Please note that a different foil with much higher O and Si contents was used for sample K. Thus this sample was excluded from figures 5, 7 and 9. The TEM grids consist of Cu leading to strong Cu X-ray peaks in the spectra (Figure 2). Consequently,

20 Cu is excluded from the further analysis and discussion. Mg is only present in a few particles. S is the major component of the volatile material surrounding the carbonaceous particles. Fe is found in the majority (~ 95 %), Cr in about 87 % and Ni in about 49 % of particles.

The spatial distribution of minor elements within the carbonaceous particles was investigated by element distribution images

25 (Figure 6) and by measuring several points on the same particle. C is the most abundant element and is contained in the whole particle. The elements O, Si, Cr and Fe only occur in some regions of the particle. The element Al is only detected in few particles. Due to the low number of X-ray counts, the distribution of Mg and Ni is difficult to assess. S seems to occur in the whole particle and is assumed to be present as surface coating of sulfate. The heterogeneous element distribution was also observed in multiple point measurements (up to 20 points on one particle).

Based on elemental composition, the refractory carbonaceous particles (number n = 330) were classified into four groups (Table 2). Only few particles consist of C, O, and Si only. Many particles contain additional Cr, Fe and Ni (n = 131) or Cr and Fe (n = 125). Particles only containing additional Fe are rare (n = 22). Please note that the element S was not used for particle

classification, because this element is found in all spectra. As all particles are either embedded in sulfates or have sulfate surface coatings it is assumed that S is not contained in the carbonaceous material.

Element ratios relative to C (at% / at%) are shown in Figure 7 for all samples. The median O/C ratio varies between 0.052 and 0.129. The median Si/C ratios vary between 0.003 and 0.012, but may be influenced by the substrate. For all other elements, the respective median ratios are generally very low (< 0.005). Sample K is not shown due to the different substrate used (with lower C and higher Si content). The differences between the various samples are for all element ratios statistically significant on the 5 % level. Most obvious, sample G has lower element/C ratios than the other samples.

TEM analysis of the particle nanostructure

The nanostructure was investigated by high resolution TEM. All particles are either completely amorphous (Figure 8 a, b) or show only very small regions (less than ten graphene sheets) with ordering (Figure 8 c, d). In the latter case, the graphene sheet separation distance was determined (Table 3). As these measurements are very time-consuming, only 44 particles from 5 samples were investigated. The graphene sheet separation distance varies between 0.19 and 0.60 nm, the mean values of different grains between 0.25 and 0.47 nm. This size range is slightly larger for both lower and upper values than typically found for soot (Vander Wal et al., 2010; Li et al., 2011; Liati et al., 2014; Weinbruch et al., 2016).

The samples, with the exception of one (sample D), were collected inside the polar vortex. Element ratios of the samples inside and outside the vortex are compared in Figure 9. There are no statistically significant differences on the 5% level in element ratios and particle size (Figure 4) between these two cases.

4. Discussion

4.1 Occurrence of refractory carbonaceous particles in the stratosphere

The major finding of the present paper is the high abundance (28-82% by number) of refractory carbonaceous particles (Figure 3), which mostly contain minor amounts of Fe, Cr and Ni heterogeneously distributed within the particles. The high abundance of refractory carbonaceous particles is in good accordance the findings of Weigel et al., 2014. With their measuring device COPAS (COndensation PArticle counting System, e.g. Weigel et al., 2009; Borrmann et al., 2010; Ebert et al., 2016) they detected a high amount of refractory particles (thermostable at 250 °C) within the polar vortex during three stratospheric campaigns (EUPLEX 2003, RECONCILE 2010 and ESSenCe 2011; Weigel et al., 2014).

Refractory carbonaceous particles in the polar stratosphere were identified in several earlier studies. Depending on the applied technique different terms were used for such particles. In the present contribution the following nomenclature is used: All particles consisting predominantly of the element carbon are termed carbonaceous, i.e., only the chemical composition is used

for classification. The term soot is used for agglomerates of primary particles (20 – 50 nm size) predominantly consisting of carbon which show a specific, onion-shell like nanostructure (Buseck et al., 2012). Black carbon (BC) is used for particles strongly absorbing light in a wide spectrum of the visible wavelength (Petzold et al., 2013) with at least 5 m^2g^{-1} at a wavelength of 550 nm (Bond et al., 2013).

5 As indicated by several publications, the presence of soot in the stratosphere was previously identified by scanning and transmission electron microscopy in accordance with the nomenclature outlined above (Pueschel et al., 1992, 1997; Sheridan et al., 1994; Blake and Kato, 1995; Strawa et al., 1999; Ebert et al., 2016). Chuan and Woods (1984) found carbonaceous particles which might be soot although they were not unequivocally identified as such, due to the lack of high resolution images. Volatile organic and amorphous particles, mainly composed of carbon, were reported by Sheridan et al. (1989). The

10 amorphous particles shown by these authors have diameters of ~2 µm. Thus, the refractory carbonaceous particles of the present paper may be of similar origin but have significantly smaller size. Sheridan et al. (1989) did not specify any potential source of these particles. Testa et al. (1990) found seven poorly graphitized carbon particles in their samples and regarded them as artifacts of carbon films from the TEM grids. As they did not provide images of these particles, they cannot be compared to our findings. However, we can exclude that our particles are substrate contaminants, since such particles did not

15 occur on the blank samples. In addition, the refractory carbonaceous particles were only observed within the impaction spot and not on the clean substrate.

Carbonaceous particles partly containing heterogeneous metallic inclusions were found by Chen et al. (1998). Some of these particles were denominated as soot without providing a more precise description. Thus, it is not clear if the "soot particles" observed by Chen et al. (1998) are similar to soot as defined by us. According to these authors, the "soot particles" most likely

20 stem from aircraft exhaust, as the samples were – at least partly – collected in the exhaust of an aircraft in the lower stratosphere. Mixed carbon-sulfur particles were observed by Nguyen et al. (2008) at 10 km altitude and were considered to have formed from condensed organic matter. However, particles differ in morphology and chemical composition from the refractory carbonaceous particles encountered in our study.

25 Stratospheric carbonaceous particles were also often detected by means of mass spectrometry (MS). For example, Murphy et al. (1998, 2013) identified carbonaceous particles, with a lower abundance in the stratosphere compared to the upper troposphere. The same group (Murphy et al., 2007) reported the presence of a small fraction of carbonaceous particles (diameter ≤ 300 nm) within the stratosphere. As some of these particles contained potassium, they were assumed to originate from biomass burning. Particles from rocket and space shuttle exhaust (collected in the stratosphere) were investigated by

30 Cziczo et al. (2002). In solid fuel rocket exhaust (Athena rocket and space shuttle boosters) the most frequent observed signals stem from different aluminum oxide species (often with minor amounts of Fe). About 17% of the particles (Athena rocket) were classified as carbonaceous as compared to 1% from space shuttle exhaust. In principle, the carbonaceous particles found by MS could be similar to the carbonaceous particles of the present study. Since MS does not yield images or information on the nanostructure, no definite conclusion can be drawn.

Stratospheric carbonaceous particles were also identified by optical measurements. For example, a single particle soot photometer (SP2) was applied by Baumgardner et al. (2004) on board of an aircraft in order to identify ozone loss processes in the polar vortex. In total, 60% of the light absorbing particles incandesce at temperatures above 3500 K and are, thus,

5   interpreted as BC. According to Baumgardner et al. (2004) these particles originate from tropospheric sources rather than aircraft emissions. The same technique was applied by Schwarz et al. (2006) to identify BC in midlatitudes from the boundary layer to the lower stratosphere. Only ≤1% of the particles was classified as BC and no potential source was specified. Local enhancements of carbonaceous material at altitudes around 25 km were also deduced from simultaneous measurements of a spectrometer on board a satellite as well as from radiance and particle counter data (Renard et al., 2008) obtained on a

10 stratospheric balloon. This material was thought to be injected into the stratosphere by the pyro-convective effect (i.e., fires that have sufficient energy to trigger convection and inject particles to the upper troposphere and lower stratosphere). Some of the particles with submicron size were supposed to originate from vaporized interplanetary material (Renard et al., 2008). Due to the lack of information on morphology, chemistry and microstructure of the particles, a direct comparison of the carbonaceous material deduced from optical measurements with the particles encountered in the present study is not possible.

In the present study, only carbonaceous particles and sulfates were observed similar to previous findings (Pueschel et al., 1992; Blake and Kato, 1995; Strawa et al., 1999; Nguyen et al., 2008). There are, however, several previous publications which describe the presence of a variety of other refractory particle groups in addition to carbonaceous particles. These additional particle groups include metallic particles (Chuan and Woods, 1984; Sheridan et al., 1994; Chen et al., 1998; Baumgardner et

20 al., 2004; Ebert et al., 2016), meteoritic particles (Murphy et al., 1998, 2007, 2013; Renard et al., 2008, Ebert et al., 2016), silicates (Testa et al., 1990; Ebert et al., 2016), crustal-type particles (Sheridan et al., 1989, 1994; Chen et al., 1998), as well as Ca-bearing particles (Sheridan et al., 1989; Della Corte et al., 2013; Ebert et al., 2016). In summary, the sole occurrence of refractory carbonaceous particles and sulfates in stratospheric samples was reported in previous literature but seems to be uncommon.

25 **4.2 Potential Sources**

The most likely sources of refractory carbonaceous particles found in the current study include aircraft emissions, extraterrestrial sources, rocket exhaust and explosive volcanic emissions as these sources emit material directly into the stratosphere. In addition, biomass burning can be considered as a possible source, as it was shown by several authors that large fires have sufficient energy to inject particles into the lower stratosphere (Fromm et al., 2000, 2006, Siebert et al., 2000;,

30 Fromm and Servranckx, 2003; Jost et al., 2004; Siddaway et al., 2011). Domestic wood burning, coal combustion, diesel engines and ship exhaust are not expected to significantly contribute to the stratospheric particle load. However, as these sources emit large amounts of carbonaceous material on a global scale (Bond et al., 2004, Gaffney and Marley, 2005, Corbett and Koehler, 2003; Lauer et al., 2007), they need to be discussed shortly. For example Thornberry et al., 2010 show that

tropical tropospheric particles contain high amounts of thermostable carbonaceous material, and it is possible that these particles become mixed within stratospheric air. Although the vertical exchange may be less effective than the direct injection processes, however, it is conceivable that fractions of carbonaceous aerosol material released in the troposphere is vertically transported into the stratosphere by processes such as tropical convection (and lifted further via the Brewer-Dobson

5   circulation), cyclogeneses, warm conveyor belts, tropopause folds and/or isentropic transport.

Aircraft exhaust

High flying aircraft can contribute significantly to the stratospheric aerosol burden. Soot is described as the main particulate exhaust component (Twohy and Gandrud, 1998; Popovitcheva et al., 2000; Smekens et al., 2005; Vander Wal et al., 2010;

10   Liati et al., 2014). The observed soot consisted of primary particles 10 - 50 nm in diameter which formed aggregates with diameters of up to approximately 450 nm (Twohy and Gandrud, 1998; Popovitcheva et al, 2000; Smekens et al., 2005; Liati et al., 2014). The nanostructure of the primary particles varied from an onion-shell structure with partial ordering (Popovitcheva et al., 2000; Vander Wal et al., 2010) to completely amorphous (Twohy and Gandrud, 1998). The mean graphene sheet separation distance of the partly ordered primary particles varied between 0.36 and 0.41 nm (Vander Wal et

15   al., 2010; Liati et al., 2014). An atomic O/C ratio of 0.32 was reported by Vander Wal et al. (2010).The elements S, Na (sodium), N (nitrogen), Zn (zinc), Ba (barium), Cl (chlorine), K (potassium), Fe and Si were detected at minor concentrations (Vander Wal et al., 2010; Mazaheri et al., 2013). In addition to soot agglomerates, single carbon spheres were found by Mazaheri et al. (2013) in aircraft exhaust. The particles have diameters between 5-100 nm with a median of 35.4 nm. Besides C, minor O, S, Cl, K, Fe and Si were detected by TEM-EDX and Proton Induced X-ray Emission (PIXE) analysis. Aircraft

20   exhaust is excluded as source of the carbonaceous particles encountered in the present study, as we did not observe soot agglomerates. In addition, the chemistry and morphology (basically rounded shapes) of the single carbon particles described by Mazaheri et al. (2013) are different from our particles.

Extraterrestrial particles

25   With an input of 5-270 tons per year (Plane, 2012), extraterrestrial material is expected to be the major source of refractory stratospheric particles (Murphy et al., 1998; 2007). Carbonaceous material is observed in chondrites as well as in interplanetary dust particles (IDPs).

In carbonaceous chondrites, a variety of different carbonaceous constituents is described in previous literature. For example, nanometer-sized carbon-rich flakes, spheres and tubes as well as hollow carbon-rich nanospheres were found (Garvie and

30   Buseck, 2004; Garvie, 2006; Garvie et al., 2008). Most carbonaceous nanospheres are amorphous. Besides C, the only other elements detected are S, N and O. Carbonaceous material in carbonaceous chondrites was also investigated by Aoki and Akai (2008). Different morphologies like "ribbon-film–like carbonaceous material", "spherical carbonaceous globules", "concentric-sphere type carbon material", and "featureless carbon material" were observed. They also describe the occurrence of minor amounts of Cl in many of these particles, an element never observed in our study. Neither morphology nor shape or

chemical composition of the particles described above is matching the refractory carbonaceous particles encountered in the present study. Carbon nanoparticles with diameters between 2-10 nm were observed in carbonaceous material isolated from the Allende carbonaceous chondrite (Harris et al., 2000). The particles had either a single outer wall or were surrounded by multiple walls. However, as the particles were mobile under the electron beam, no photographs are shown. A comparison to our particles is thus difficult. Since the authors did not find any other elements except C, most of our particles differ in chemical composition as they contain Fe, Cr, and/or Ni as minor elements.

Carbonaceous material was also found in IDPs (Matrajt et al., 2012). Some of the material observed is similar in size, morphology and nanostructure to our particles. However, in Matrajt et al. (2012) minor elements were not investigated and this parameter cannot be compared.

In summary, the carbonaceous components observed in chondrites differ in chemical composition from most of our particles. Carbonaceous material contained in IDPs cannot be excluded as source of the refractory particles encountered in the present study, as the minor element concentration of the former is not known. However, if we expect extraterrestrial material to be the major source of our particles, we would also expect to find Mg-rich silicates in our samples, which was not the case. Furthermore, the occurrence of Fe, Cr and Ni as minor elements in our refractory carbonaceous particles is regarded as hint for an anthropogenic origin. This interpretation is supported by the fact that the observed average atomic ratios of these three elements (Cr/Fe = 0.249, Ni/Fe = 0.167, Cr/Ni = 1.145) are significantly higher than the cosmic element ratios (Cr/Fe = 0.015, Ni/Fe = 0.056, Cr/Ni = 0.278; Palme and Jones, 2005).

Rocket Exhaust

Rocket exhaust is also a possible source of stratospheric particles. However, literature on particles emitted by rockets is sparse (e.g. Zolensky et al., 1989), and there are – to the best of our knowledge – no studies available on carbonaceous particles by electron microscopy. According to Ross and Sheaffer (2014), five different propellant types which use a combination of different oxidizers and fuels are in use: O_2/kerosene, O_2/H_2, NH_4ClO_4/Al, N_2H_4/N_2O_4 and N_2O/solid hydrocarbons. Solid rocket motors (SRM) emit characteristic Al_2O_3 spheres (Strand et al., 1981; Zolensky et al., 1989; Cofer III et al., 1991) and can, thus, be excluded as source of the carbonaceous particles encountered in the present study. Hydrocarbon-fired rockets are powered by kerosene or syntin and can be expected to emit soot. For example, soot particles most likely emitted by a Russian Soyuz booster rocket were found in an aerosol cloud at 20 km (Newman et al., 2001). The soot particles comprised approximately 1/4 to the total particle number, the rest were volatile sulfate particles. The occurrence of carbonaceous material from rocket exhaust was also reported by Cziczo et al. (2002). In the exhaust of an Athena II rocket, the carbonaceous fraction of material was found to be 17% by number (Cziczo et al., 2002). The refractory carbonaceous particles observed by us may in principle originate from rocket exhaust, which could also explain the occurrence of the minor elements Fe, Cr and Ni (rocket debris). However, as carbonaceous rocket exhaust particles were not investigated previously by electron microscopy this question remains open.

Volcanic emissions

Volcanic eruptions are generally not considered to emit carbonaceous material. However, carbonaceous material was found in samples from the Kasatochi (Alaska, 2008), Sarychev (Russia, 2009) as well as Eyafjallajökull (Island, 2010) eruptions (Martinsson et al., 2009; Schmale et al.; 2010; Andersson et al., 2013). The carbonaceous material most probably originates

5 from air entrained into the volcanic cloud. The carbonaceous mass fraction in plumes from two volcanoes in Ecuador and Columbia was found to vary between 19-38% (measured by MS; Carn et al., 2011). Sulfur-carbonaceous mixed particles occurred predominantly in the size range below 0.9 µm. In 1999, the year before the campaign, there were four volcanic eruptions with a VEI ≥ 4 (Volcanic Explosivity Index): Soufrière Hills (West Indies) in January, Shiveluch (Russia) in August as well as Guagua Pichincha (Ecuador) and Tungurahua (Ecuador) in October (NOAA, 2017). Still, volcanism seems an

10 unlikely source for our samples, as volcanic eruptions will emit large amounts of silicate particles, which we did not observe.

Biomass burning

A further source of carbonaceous particles in the stratosphere is biomass burning (BB). Particles originating from BB can be lifted to the stratosphere by either the tropical upper tropospheric upwelling or the pyroconvective effect (Fromm et al., 2000;

15 Jost et al., 2004). Three different types of carbonaceous BB particles were described in previous literature (e.g., Pósfai et al., 2003; 2004; Kis et al., 2006; Li and Shao, 2009): organic particles with inorganic inclusions, tar ball particles and soot. Organic particles (no specific morphology) contain C and minor O, and are stable under the electron beam. They do not show the typical microstructure of soot (see below). The inorganic inclusions mostly consist of KCl and K_2SO_4. Tar balls have a typical spherical shape and mainly consist of C and O with minor K, S, Cl and Si contents. Soot consists of chain-like agglomerates

20 of primary particles (10 – 100 nm) with a typical onion shell microstructure (graphene sheet separation distance between 0.133 and 0.137 nm). As our particles do not show the characteristics of all types of carbonaceous BB particles described above, this source can be excluded.

The most probable potential sources for carbonaceous particles were already discussed above. For these sources the transport

25 mechanisms into the stratosphere are well known. There are further strong tropospheric sources for carbonaceous particles, which predominately emit particles at ground level. An effective transport to the stratosphere of these particles is unlikely. Still, they will be discussed briefly, as they are – on a global scale – major sources of carbonaceous material in the lower atmosphere.

30 *Wood burning*

Soot is a major component emitted by wood burning. Similar to biomass burning, soot from wood burning consists of agglomerates of spherical primary particles (20 – 80 nm diameter) with an onion-shell nanostructure (Kocbach et al., 2005; Torvela et al., 2014, Tumolva et al., 2010). Some primary particles are amorphous (Tumolva et al., 2010). The particles may have a surface coating which is volatile under electron bombardment (Torvela et al., 2014). Carbon is the major element of

wood burning soot, O, Na, Si, S, Cl, K, and Ca occur as minor elements (Kocbach et al., 2005; Tumolva et al., 2010). In addition to soot, particulate organic matter (POM) was found in wood burning (Torvela et al., 2014). The POM particles, sometimes described as tar balls are 30 - 600 nm in diameter. Judged from the properties described above, both soot and POM are different to the particles observed in our study. Thus, wood burning can be excluded as a source for the refractory
5   carbonaceous stratospheric particles.

Coal burning

A variety of different carbonaceous particles was observed during coal burning. Most carbonaceous particles are soot particles, i.e., fractal-like agglomerates (0.1 – 1 µm size) consisting of 10 – 50 nm diameter primary particles. The primary particles
10   show a characteristic onion-shell structure (Chen et al., 2004, 2005). Some of the soot agglomerates have inorganic inclusions or inorganic particles on their surface, containing Mg, Ca, Sr (strontium), Ba (barium) and Na (Chen et al., 2005). Char particles associated with ultrafine titanium oxide particles were also found (Chen et al., 2005). Sometimes ultrafine Ti, Al, Fe and Ca particles were embedded in large char particles. In addition, graphitic fiber structures that are either straight or curved were encountered. Two of the three types of carbonaceous particles described for coal combustion (soot agglomerates and graphitic
15   fibers) are certainly different from our particles. As images of char particles were not provided by Chen et al. (2005) we cannot compare their results to the refractory carbonaceous particles of the present study. We regard coal combustion as an implausible source.

Diesel engines

20   Diesel engines are another important source of carbonaceous particles and above all soot particles. Again, soot agglomerates consist of spherical primary particles (5 – 50 nm diameter) with onion-shell nanostructure (e.g., Tumolva et al., 2010; Wentzel et al., 2010; Li et al. , 2011; Song, 2004; Weinbruch et al., 2016). The graphene sheet separation distance varies between 0.31 – 0.48 nm; (Vander Wal et al., 2010; Li et al., 2011; Weinbruch et al., 2016), and the intensity O/C ratio between 0.049 – 0.079 (Weinbruch et al., 2016). Compared to our particles, the chemical composition, morphology and primary particle size of diesel
25   exhaust particles are significantly different. Thus, we can certainly exclude this source.

Ship emissions

Ship emissions also contain soot agglomerates (Popovicheva et al., 2012; Lieke et al., 2013). Their chemical composition is dominated by C and O, with small amounts (< 1 wt %) of additional elements; e.g. V, S, Cl, Ca and Si (Popovicheva et al.,
30   2012). Furthermore, spherical char particles with diameters of 0.2 – 1 µm are found to be characteristic for ship emissions (Popovicheva et al., 2012). The morphology of these particles shown in SEM photomicrographs is different to the particles found in our study. Lieke et al., 2013 found amorphous carbonaceous material filling cavities of larger soot aggregates. The characteristics described for ship exhaust particles are significantly different to the particles found in our study, leading to the conclusion that that ship exhaust can be excluded as the source.

5. Summary

The major finding of the present study is the exceptional high abundance of refractory carbonaceous particles collected in and outside of the stratospheric polar vortex. By number, up to 82 % of the particles were found to be externally mixed refractory carbonaceous particles. In addition, approximately 10% of the particles are internal mixtures of refractory carbonaceous particles and sulfates. Most of the carbonaceous particles show small and variable amounts of the elements Fe, Cr and Ni. The exact source of the refractory carbonaceous particles remains unclear and can only be confined by exclusion. The most likely sources are rocket exhaust and extraterrestrial material.

Data availability. The data set is available for the community and can be accessed by request to Katharina Schütze (schuetze@geo.tu-darmstadt.de) of the Technische Universität Darmstadt.

Author contributions. Katharina Schütze analyzed the samples, interpreted the data and prepared the manuscript. Nathalie Benker supported the TEM analysis. Martin Ebert came up with suggestions for and supported the SEM analysis. Stephan Weinbruch contributed to the preparation of the manuscript and came up with ideas of interpretation and analysis. Stephan Borrmann and Ralf Weigel supported the scope of the analysis as well as interpretation of data and writing. James C. Wilson provided the samples as well as any necessary date regarding the sampling campaign, contributed to the data analysis, interpretation and writing.

Competing interests. All authors declare that they have no conflict of interest.

Acknowledgements. Our research was funded by the European Research Council under FP7 (FP/2007-2013)/ERC grant agreement no. 321040 (EXCATRO). This work was partly supported by the project ROMIC-SPITFIRE sponsored by the Federal Ministry of Education and Research (FKZ 01LG1205D) and by STRATOCLIM sponsored by the European Union Seventh Framework Programme (FP7), project reference 603557.

References

Andersson, S. M., Martinsson, B. G., Friberg, J., Brenninkmeijer, C. A. M., Rauthe-Schöch, A., Hermann, M., van Velthoven, P. F. J., and Zahn, A.: Composition and evolution of volcanic aerosol from eruptions of Kasatochi, Sarychev and Eyjafjallajökull in 2008-2010 based on CARIBIC observations, Atmos. Chem. Phys., 13, 1781-1796, doi:10.5194/acp-13-1781-2013, 2013.

Aoki, T. and Akai, J.: Carbon materials in Antarctic and nonAntarctic carbonaceous chondrites: high-resolution transmission electron microscopy, J. Miner. Petrol. Sci., 103, 173-182, doi:10.2465/jmps.070301, 2008.

Arnold, F., Curtius, J., Spreng, S., and Deshler, T.: Stratospheric aerosol sulfuric acid: First direct in situ measurements using a novel balloon-based mass spectrometer apparatus, J. Atmos. Chem., 30, 3-10, doi:10.1023/A:1006067511568, 1998.

Austin, J., and Li, F.: On the relationship between the strength of the Brewer-Dobson circulation and the age of stratospheric air, Geophys. Res. Lett., 33, L17807, doi:10.1029/2006GL026867, 2006.

Baumgardner, D., Kok, G., and Raga, G.: Warming of the Arctic lower stratosphere by light absorbing particles, Geophys. Res. Lett., 31, L06117, doi:10.1029/2003GL018883, 2004.

Bigg, E. K., Ono, A., and Thompson, W. J.: Aerosols at altitudes between 20 and 37 km, Tellus, 22, 550-563, doi:10.1111/j.2153-3490.1970.tb00522.x ,1970.

Bigg, E. K.: Stratospheric Particles, J. Atmos. Sci., 32, 910-917, 1975.

Bigg, E. K.: Sources of insoluble inclusions in stratospheric sulfate particles, Meteorit. Planet. Sci., 47, 799–805, doi:10.1111/j.1945-5100.2012.01346.x, 2012.

Blake, D. F. and Kato, K.: Latitudinal distribution of black carbon soot in the upper troposphere and lower stratosphere, J. Geophys. Res., 100, 7195-7202, doi:10.1029/94JD03118, 1995.

Bond, T. C., Streets, D. G., Yarber, K. F., Nelson, S. M., Woo, J.-H., and Klimont, Z.: A technology-based global inventory of black and organic carbon emissions from combustion, J. Geophys. Res. 109, D14203, doi:10.1029/2003JD003697, 2004.

Bond, T. C., Doherty, S. J., Fahey, D. W., Forster, P. M., Berntsen, T., DeAngelo, B. J., Flanner, M. G., Ghan, S., Kärcher, B., Koch, D., Kinne, S., Kondo, Y., Quinn, P. K., Sarofim, M. C., Schultz, M. G., Schulz, M., Venkataraman, C., Zhang, H., Zhang, S., Bellouin, N., Guttikunda, S. K., Hopke, P. K., Jacobson, M. Z., Kaiser, J. W., Klimont, Z., Lohmann, U., Schwarz, J. P., Shindell, D., Storelvmo, T., Warren, S. G., and Zender, C. S.: Bounding the role of black carbon in the climate system: A scientific assessment, J. Geophys. Res.: Atmos., 118, 5380-5552, 2013.

Borrmann, S., Kunkel, D., Weigel, R., Minkin, A., Deshler, T., Wilson, J. C., Curtius, J., Volk, C. M., Homan, C. d., Ulanovsky, A., Ravegnani, F., Viciani, S., Shur, G. N., Belyaev, G. V., Law, K. S., and Cairo, F.: Aerosols in the tropical and subtropical UT/LS: in-situ measurements of submicron particle abundance and volatility, Atmos. Chem. Phys., 10, 5573-5592, doi:10.5194/acp-10-5573-2010, 2010.

Brownlee, D. E.: Cosmic dust: collection and research, Ann. Rev. Earth Planet. Sci., 13, 17-143, 1985.

Buseck, P. R., Adachi, K., Gelencsér, A., Tompa, É., and Pósfai, M.: Are black carbon and soot the same?, Atmos. Chem. Phys. Discuss., 12, 24821-24846, doi:10.5194/acpd-12-24821-2012, 2012.

Carn, S. A., Froyd, K. D., Anderson, B. E., Wennberg, P., Crounse, J., Spencer, K., Dibb, J. E., Krotkov, N. A., Browell, E. V., Hair, J. W., Diskin, G., Sachse, G., and Vay, S. A.: In situ measurements of tropospheric volcanic plumes in Ecuador and Colombia during TC[4], J. Geophys. Res., 116, D00J24, doi:10.1029/2010JD014718, 2011.

Chen, Y., Kreidenweis, S. M., McInnes, L. M., Rogers, D. C., and DeMott, P. J.: Single particle analyses of ice nucleating aerosols in the upper troposphere and lower stratosphere, Geophys. Res. Lett., 25, 1391–1394, 1998.

Chen, Y, Shah, N., Huggins, F. E., Huffman, G. P., Linak, W. P., and Miller, C. A.: Investigation of primary fine particulate matter from coal combustion by computer-controlled scanning electron microscopy, Fuel. Process. Technol., 85, 743-761, doi:10.1016/j.fuproc.2003.11.017, 2004.

Chen, Y., Shah, N., Huggins, F. E., and Huffman, G. P.: Transmission electron microscopy investigation of ultrafine coal fly ash particles, Environ. Sci. Technol., 39, 1144-1151, 2005.

Chuan, R. L. and Woods, D. C.: The appearance of carbon aerosol particles in the lower stratosphere, Geophys. Res. Lett., 11, 553-556, 1984.

Cofer III, W. R., Purgold, G. C., Winstead, E. L., and Edahl, R. A.: Space shuttle exhausted aluminum oxide: A measured particle size distribution, J. Geophys. Res.-Atmos., 96, 17371–17376, 1991.

Corbett, J. J., and Koehler, H. W.: Updated emissions from ocean shipping, J. Geophys. Res., 108, 4650, doi:10.1029/2003JD003751, 2003.

Cziczo, D. J., Thomson, D. S., and Murphy, D. M.: Ablation, flux, and atmospheric implications of meteors inferred from stratospheric aerosol, Science, 291, 1772–1775, 2001.

Cziczo, D. J., Murphy, D. M., Thomson, D. S., and Ross, M. N.: Composition of individual particles in the wakes of an Athena II rocket and the space shuttle, Geophys. Res. Lett., 29, 2037, doi:10.1029/2002GL015991, 2002.

Cziczo, D. J., Froyd, K. D., Hoose, C., Jensen, E. J., Diao, M., Zondlo, M. A., Smith, J. B., Twohy, C. H., and Murphy, D. M.: Clarifying the Dominant Sources and Mechanisms of Cirrus Cloud Formation, Science, 340, 1320-1324, 2013.

Della Corte, V., Rietmeijer, F. J. M., Rotundi, A., Ferrari, M., and Palumbo, P.: Meteoric CaO and carbon smoke particles collected in the upper stratosphere from an unanticipated source, Tellus B, 65, 20174, doi:10.3402/tellusb.v65i0.20174, 2013.

Ebert, M., Weigel, R., Kandler, K., Günther, G., Molleker, S., Grooß, J.-U., Vogel, B., Weinbruch, S., and Borrmann, S.: Chemical analysis of refractory stratospheric aerosol particles collected within the arctic vortex and inside polar stratospheric clouds, Atmos. Chem. Phys., 16, 8405-8421, doi:10.5194/acp-16-8405-2016, 2016.

Engel, I., Luo, B. P., Pitts, M. C., Poole, L. R., Hoyle, C. R., Grooß, J.-U., Dörnbrack, A., and Peter, T.: Heterogeneous formation of polar stratospheric clouds – Part 2: Nucleation of ice on synoptic scales, Atmos. Chem. Phys., 13, 10769–10785, doi:10.5194/acp-13-10769-2013, 2013.

Fahey, D.W., Keim, E. R., Boering, K. A., Brock, C. A., Wilson, J. C., Jonsson, H., Anthony, S., Hanisco, T. F., Wennberg, P., Miake-Lye, R. C., Salawitch, R., Louisnard, N., Woodbridge, E. L., Gao, R. S., Donnelly, S., Wamsley, R. C., Del Negro,

L. A., Solomon, S., Daube, B. C., Wofsy, S. C., Webster, C. R., May, R. D., Kelly, K. K., Loewenstein, M., Podolske, J. R., and Chan, K. R.: Emission measurements of the Concorde supersonic aircraft in the lower stratosphere. Science 270, 70–74, doi:10.1126/science.270.5233.70, 1995.

Frankland, V. L., James, A. D., Feng, W., and Plane, J. M. C.: The uptake of HNO3 on meteoric smoke analogues, J. Atmos. Sol.- Terr. Phys., doi:10.1016/j.jastp.2015.01.010, 2015.

Fromm, M., Alfred, J., Hoppel, K., Hornstein, ., Bevilacqua, R., Shettle, E., Servranckx, R., Li, Z., and Stocks, B.: Observations of boreal forest fire smoke in the stratosphere by POAM III, SAGE II, and lidar in 1998, Geophys. Res. Lett., 27, 1407-1410, doi:10.1029/1999GL011200, 2000.

Fromm, M. D., and Servranckx, R.: Transport of forest fire smoke above the tropopause by supercell convection, Geophys. Res. Lett., 30, 1542, doi:10.1029/2002GL016820, 2003.

Fromm, M., Tupper, A., Rosenfeld, D., Servranckx, R., and McRae, R.: Violent pyro-convective storm devastates Australia's capital and pollutes the stratosphere, Geophys. Res. Lett., 33, L05815, doi:10.1029/2005GL025161, 2006.

Gaffney, J. S., and Marley, N. A.: The impacts of combustion emissions on air quality and climate – From coal to biofuels and beyond, Atmos. Environ., 42, 23-36, doi:10.1016/j.atmosenv.2008.09.016., 2009.

Garvie, L. A. J. and Buseck, P. R.: Nanosized carbon-rich grains in carbonaceous chondrite meteorites, Earth Planet. Sci. Lett., 224 (3-4), 431-439, doi:10.1016/j.epsl.2004.05.024, 2004.

Garvie, L. A. J.: Extraterrestrial carbon nanospheres, Carbon, 44, 158-160, doi:10.1016/j.carbon.2005.08.028, 2006.

Garvie, L. A. J., Baumgardner, G., and Buseck, P. R.: Scanning electron microscopical and cross sectional analysis of extraterrestrial carbonaceous nanoglobules, Meteorit. Planet. Sci., 43, 899–903. doi:10.1111/j.1945-5100.2008.tb01088.x, 2008.

Greenblatt, J. B., Jost, H.-J., Loewenstein, M., Podolske, J. R., Hurst, D. F., Elkins, J. W., Schauffler, S. M., Atlas, E. L., Herman, R. L., Webster,, C. R., Bui, T. B., Moore, F. L., Ray, E. A., Oltmans, S., Vömel, H., Blavier, J.-F., Sen, B., Stachnik, R. A., Toon, G. C., Engel, A., Müller, M., Schmidt, U., Bremer, H., Pierce, R. B., Sinnhuber, B.-M., Chipperfield, M., and Lefèvre, F.: Tracer-based determination of vortex descent in the 1999/2000 Arctic winter, J. Geophys. Res., 107, 8279, doi:10.1029/2001JD00937, 2002.

Harris, P. J. F., Vis, R. D., and Heymann, D.: Fullerene-like carbon nanostructures in the Allende meteorite, Earth Planet. Sci. Lett., 183, 355-359, doi:10.1016/S0012-821X(00)00277-6, 2000.

Harris, P. J. F.: Carbonaceous contaminants on support films for transmission electron microscopy, Carbon, 39, 909-913, doi:10.1021/nn9001598, 2001.

Helsel, D. R.: Statistics for Censored Environmental Data Using Minitab® and R, John Wiley & Sons, Hoboken, New Jersey, 2012, 324 pp.

Holton, J. R., Hayes, P. H., McIntyre, M. E., Douglass, A. R., Rood, R. B., and Pfister, L.: Stratosphere-Troposphere exchange, Rev. Geophys., 33, 403-439, 1995.

Hoyle, C. R., Engel, I., Luo, B. P., Pitts, M. C., Poole, L. R., Grooß, J.-U., and Peter, T.: Heterogeneous formation of polar stratospheric clouds – Part 1: Nucleation of nitric acid trihydrate (NAT), Atmos. Chem. Phys., 13, 9577-9595, 2013.

Hunten, D. M., Turco, R. P., and Toon, O. W.: Smoke and dust particles of meteoric origin in the mesosphere and stratosphere, J. Atmos. Sci., 37, 1342-1357, 1980.

5 Rasband, W. S., ImageJ, U. S. National Institutes of Health, Bethesda, Maryland, USA, http://imagej.nih.gov/ij/, 1997-2016.

Jost, H.-J., Loewenstein, M., Greenblatt, J. B., Podolske, J.R., Bui, T. P., Hurst, D. F., Elkins, J. W., Herman, R. L., Webster, C. R., Schauffler, S. M., Atlas, E. L., Newman, P. A., Lait, L. R., and Wofsy, S. C.: Mixing events revealed by anomalous tracer relationships in the Arctic vortex during winter 1999/2000, J. Geophys. Res., 107, 4795, doi:10.1029/2002JD002380, 2002.

10 Jost, H.-J., Drdla, K., Stohl, A., Pfister, L., Loewenstein, M., Lopez, J. P., Hudson, P. K., Murphy, D. M., Cziczo, D. J., Fromm, M., Bui, T. P., Dea-Day, J., Gerbig, C., Mahoney, M. J., Richard, E. C., Spichtinger, N., Vellovic Pittman, J., Weinstock., E. M., Wilson, J. C., and Xueref, I.: In-situ observations of mid-latitude forest fire plumes deep in the stratosphere, Geophys. Res. Lett., 31, L11101, doi:10.1029/2003GL019253, 2004.

Junge, C. E., Changnon, C. W., And Manson, J. E., Stratospheric aerosols, J. Meteorol., 18, 81-108, 1961.

15 Junge, C. E., and Manson, J. E.: Stratospheric aerosol studies, J. Geophys. Res., 66, 2163-2182, doi:10.1029/JZ066i007p02163, 1961.

Junge, C. E.: Sulfur in the atmosphere, J. Geophys. Res., 68, 3975-3976, doi:10.1029/JZ068i013p03975, 1963.

Kis, V. K., Pósfai, M., and Lábár, J. L.: Nanostructure of atmospheric soot particles, Atmos. Environ., 40, 5533-5542, doi:10.1016/j.atmosenv.2006.05.012, 2006.

20 Kocbach, A., Johansen, B. V., Schwarze, P. E., and Namork, E.: Analytical electron microscopy of combustion particles: a comparison of vehicle exhaust and residential wood smoke, Sci. Total Environ., 346,231-243, doi:10.1016/j.scitotenv.2004.10.025, 2005.

Kojima, T., Buseck, P. R., Wilson, J. C., Reeves, J. M., and Mahoney, M. J.: Aerosol particles from tropical convective systems: Cloud tops and cirrus anvils, J. Geophys. Res., 109, D12201, 2004.

25 Kojima, T., Buseck, P. R., and Reeves, J. M.: Aerosol particles from tropical convective systems: 2. Cloud bases, J. Geophys. Res., 110, D09203, 2005.

Kremser, S., Thomason, L. W., von Hobe, M., Hermann, M., Deshler, T., Timmreck, C., Toohey, M., Stenke, A., Schwarz, J. P., Weigel, R., Fueglistaler, S., Prata, F. J., Vernier, J.-P., Schlager, H., Barnes, J. E., Antuña-Marrero, J.-C., Fairlie, D., Palm, M., Mahieu, E., Notholt, J., Rex, M., Bingen, C., Vanhellemont, F., Bourassa, A., Plane, J. M. C., Klocke, D., Carn, S. A.,

30 Clarisse, L., Trickl, T., Neely, R., James, A. D., Rieger, L., Wilson, J. C., and Meland, B.: Stratospheric aerosol – Observations, processes, and impact on climate, Rev. Geophys., 54, 278-335, doi:10.1002/2015RG000511, 2016.

Lauer, a., Eyring, V., Hendricks, J., Jöckel, P., and Lohmann, U.: Global model simulations of the impact of ocean-going ships on aerosols, clouds, and the radiation budget, Atmos. Chem. Phys., 7, 5061-5079, doi:10.5194/acp-7-5061-2007, 2007.

Lee, L.: NADA: Nondetects And Data Analysis for environmental data. R package version 1.5-6. https://CRAN.R-project.org/package=NADA, 2013.

Li; W. and Shao, L.: Transmission electron microscopy study of aerosol particles from the brown hazes in northern China, J. Geophys. Res., 114, D09302, doi:10.1029/2008JD011285, 2009.

Li, Z., Song, C., Song, J., Lv, G., Dong, S., and Zaho, Z.: Evolution of the nanostructure, fractal dimension and size of in-cylinder soot during diesel combustion process, Combust. Flame, 158, 1624-1630, doi:10.1016/j.combustflame.2010.12.006, 2011.

Liati, A., Brem, B. T., Durdina, L., Vögtli, M., Dasilva, Y. A. R., Eggenschwiler, P. D., and Wang, J.: Electron microscopic study of soot particulate matter emissions from aircraft turbine engines, Environ. Sci. Technol., 48, 10975−10983, doi:10.1021/es501809b, 2014.

Lieke, K. I., Rosenørn, T., Pedersen, J., Larsson, D., Kling, J., Fuglsang, K., and Bilde, M.: Micro-and Nanostructural Characteristics of Particles Before and After an Exhaust Gas Recirculation System Scrubber, Aerosol Sci. Technol., 47, 1038-1046, doi:10.1080/02786826.2013.813012, 2013.

Manney, G. L. and Sabutis, J. L.: Development of the polar vortex in the 1999-2000 Arctic winter stratosphere, Geophys. Res. Lett., 27, 2589-2592, 2000.

Martinsson, B. G., Brenninkmeijer, C. A. M., Carn, S. A., Hermann, M., Heue, K.-P., van Velthoven, P. F. J., and Zahn, A.; Influence of the 2008 Kasatochi volcanic eruption on sulfurous and carbonaceous aerosol constituents in the lower stratosphere, Geophys. Res. Lett., 36, L12813, doi:10.1029/2009GL038735, 2009.

Matrajt, G., Messenger, S., Brownlee, D., and Joswiak, D.: Diverse forms of primordial organic matter identified in interplanetary dust particles, Meteorit. Plant. Sci., 47, 525-549, doi:10.1111/j.1945-5100.2011.01310.x, 2012.

Mattis, I., Siefert, P., Müller, D., Tesche, M., Hiebsch, A., Kanitz, T., Schmidt, J., Finger, F., Wandinger, U., and Ansmann, A.: Volcanic aerosol layers observed with multiwavelength Raman lidar over central Europe in 2008-2009, J. Geophys. Res., 115, D00L04, doi:10.1029/2009JD013472, 2010.

Mazaheri, M., Bostrom, T. E., Johnson, G. R., Morawska, L.: Composition and morphology of particle emissions from in-use aircraft during takeoff and landing, Environ. Sci. Technol., 47, 5235− 5242, doi:10.1021/es3046058, 2013.

Mossop, S. C.: Stratospheric Particles at 20 km, Science, 4891, 325-326, 1963.

Mossop, S. C.: Stratospheric particles at 20 km altitude, Geochim. Cosmochim. Ac., 29, 201-207, 1965.

Murphy, D. M., Thomson, D. S., and Mahoney, M. J.: In Situ Measurements of Organics, Meteoritic Material, Mercury, and Other Elements in Aerosols at 5 to 19 Kilometers, Science, 282, 1664−1669, doi:10.1126/science.282.5394.1664, 1998.

Murphy, D.M., Cziczo, D.J., Hudson, P.K. and Thomson, D.S.: Carbonaceous material in aerosol particles in the lower stratosphere and tropopause region, J. Geophys. Res., 112, D04203, 2007.

Murphy, D. M., Froyd, K. D., Schwarz, J. P., and Wilson, J. C.: Observations of the chemical composition of stratospheric aerosol particles, Q. J. Roy. Meteor. Soc., 140, 1269−1278, doi:10.1002/qj.2213, 2013.

Newman, P. A., Harris, N. R. P., Adriani, A., Amanatidis, G. T., Anderson, J. G., Braathen, G. O., Brune, W. H., Carslaw, K. S., Craig, M. S., DeCola, P. L., Guirlet, M., Hipskind, R. S., Kurylo, M. J., Küllman, H., Larsen, N., Mégie, G. J., Pommereau, J.-P., Poole, L. R., Schoeberl, M. R., Stroh, F., Toon, O. B., Trepte, C. R., and Van Roozendael, M.: An overview of the SOLVE/THESEO 2000 campaign, J. Geophys. Res., 107, 8259, doi:10.1029/2001JD001303, 2002.

Newman, P. A., Wilson, J. C., Ross, M. N., Brock, C. A., Sheridan, P. J., Schoeberl, M. R., Lait, L. R., Bui, T. P., Loewenstein, M., and Podolske, J. R.: Chance encounter with a stratospheric kerosene rocket plume from Russia over California, Geophys. Res. Lett., 28, 959–962, doi:10.1029/2000GL011972, 2001.

Nguyen, H. N., Martinsson, B. G., Wagner, J. B., Carlemalm, E., Ebert, M., Weinbruch, S., Brenninkmeijer, C. A. M., Heintzenberg, J., Hermann, M., Schuck, T., van Velthoven, P. F. J., and Zahn, A.: Chemical composition and morphology of individual aerosol particles from a CARIBIC flight at 10 km altitude between 50°N and 30°S, J. Geophys. Res., 113, D23209, doi:10.1029/2008JD009956, 2008.

NOAA:
https://www.ngdc.noaa.gov/nndc/struts/results?type_15=Like&query_15=&op_30=eq&v_30=&ge_23=&le_23=&op_29=eq&v_29=&type_16=Like&query_16=&le_17=&ge_18=&le_18=&ge_17=&op_20=eq&v_20=&ge_7=&le_7=&bt_24=&st_24=&type_25=EXACT&query_25=None+Selected&bt_26=&st_26=&type_27=EXACT&query_27=None+Selected&type_12=Exact&query_12=&type_11=Exact&query_11=&t=102557&s=50&d=50, last accessed January 31st 2017.

Palme, H., and Jones, A.: Solar system abundances of the elements, in: Meteorites, Comets, and Planets (ed. A. M. Davis), Treatise on Geochemistry Vol. 1, 41-61, Elsevier-Pergamon, Oxford, 2005.

Peter, T.: Microphysics and heterogeneous chemistry of polar stratospheric clouds, Annu. Rev. Phys. Chem., 48, 785-822, doi:10.1146/annurev.physchem.48.1.785, 1997.

Peter, T. and Grooß, J. U.: Polar Stratospheric Clouds and Sulfate Aerosol Particles: Microphysics, Denitrification and Heterogeneous Chemistry, chap. 4, RSC Publishing, Cambridge, 2012.

Petzold, A., Döpelheuer, A., Brock, C. A., and Schröder, F.: In situ observations and model calculations of black carbon emission by aircraft at cruise altitude, J. Geophys. Res., 104, 22171-22181, doi:10.1029/1999JD900460, 1999.

Petzold, A., Ogren, J. A., Fiebig, M., Laj, P., Li, S.-M., Baltensperger, U., Holzer-Popp, T., Kinne, S., Pappalardo, G., Sugimoto, N., Wehrli, C., Wiedensohler, A., and Zhang, X.-Y.: Recommendations for reporting „black carbon" measurements, Atmos. Chem. Phys., 13, 8365-8379, doi:10.5194/acp-13-836-2013, 2013.

Plane, J. M. C.: Cosmic dust in the earth's atmosphere, Chem. Soc. Rev., 41, 6507–6518, doi:0.1039/c2cs35132c, 2012.

Popovitcheva, O. B., Persiantseva, N. M., Trukhin, M. E., Rulev, G. B., Shonija, N. K., Buriko, Y. Y., Starik, A. M., Demirdjian, B., Ferry, D., and Suzanne, J.: Experimental characterization of aircraft combustor soot: Microstructure, surface area, porosity and water adsorption, Phys. Chem. Chem. Phys., 19, 4421-4426, doi:10.1039/B004345L, 2000.

Popovicheva, O., Kireeva, E., Persiantseva, N., Timofeev, M., Bladt, H., Ivleva, N. P., Niessner, R., and Moldanová, J.; Microscopic characterization of individual particles from multicomponent ship exhaust, J. Environ. Monit., 14, 3101, doi:10.1039/c2em30338h, 2012.

Pósfai, M., Simonics, R., Li, J., Hobbs, P. V., Buseck, P. R.: Individual aerosol particles from biomass burning in southern Africa: 1. Compositions and size distributions of carbonaceous particles, J. Geophys. Res., 108, 8483, doi:10.1029/2002JD002291, 2003.

Pósfai, M., Gelencsér, A., Simonics, R., Arató, K., Li, J., Hobbs, R. V., and Buseck, P. R.: Atmospheric tar balls: Particles from biomass and biofuel burning, J. Geophys. Res., 109, D06213, doi:10.1029/2003JD004169, 2004.

Pueschel, R. F., Blake, D. F., Snetsinger, K. G., Hansen, A. D. A., Verma, S., and Kato, K.: Black carbon (soot) aerosol in the lower stratosphere and upper troposphere, Geophys. Res. Lett., 19, 1659-1662, doi:10.1029/92GL01801, 1992.

Pueschel, R. F., Boering, K. A., Verma, S., Howard, S. D., Ferry, G. V., Goodman, J., Allen, D. A., and Hamill, P.: Soot aerosol in the lower stratosphere: Pole-to-pole variability and contributions by aircraft, J. Geophys. Res. 102, 13113-13118, doi:10.1029/96JD03061 ,1997.

R Core Team. R: A language and environment for statistical computing. R Foundation for Statistical Computing, Vienna, Austria, version 3.3.0, URL https://www.R-project.org/, 2016.

Renard, J.-B., Brogniez, C., Berthet, G., Bourgeois, Q., Gaubicher, B., Chartier, M., Balois, J.-Y., Verwaerde, C., Auriol, F., Francois, P., Daugeron, D., and Engrand, C.: Vertical distribution of the different types of aerosols in the stratosphere: Detection of solid particles and analysis of their spatial variability, J. Geophys. Res., 113, D21303, doi:10.1029/2008JD010150, 2008.

Rietmeijer, F. J. M., Della Corte, V., Ferrari, M., Rotundi, A., and Brunetto, R.: Laboratory analyses of meteoric debris in the upper stratosphere from settling bolide dust clouds, Icarus, 255, 217-234, 2016.

Rosen, J. M.: The Boiling Point of Stratospheric Aerosols, J. Appl. Meteorol., 10, 1044-1046, 1971.

Ross, M. N. and Sheaffer, P. M.: Radiative forcing caused by rocket engine emissions, Earth's Future, 2, 177-196, doi:10.1002/2013EF000160, 2014.

Saunders, R. W., Möhler, O., Schnaiter, M., Benz, S., Wagner, R., Saathoff, H., Connolly, P. J., Burgess, R., Murray, B. J., Gallagher, M., Wills, R., and Plane, J. M. C.: An aerosol chamber investigation of the heterogeneous ice nucleating potential of refractory nanoparticles, Atmos. Chem. Phys., 10, 1227–1247, doi:10.5194/acp-10-1227-2010, 2010.

Schmale, J., Schneider, J., Jurkat, T., Voigt, C., Kalesse, H., Rautenhaus, M., Lichtenstern, M., Schlager, H., Ancellet, G., Arnold, F., Gerding, M., Mattis, I., Wendisch, M., and Borrmann, S.: Aerosol layers from the 2008 eruptions of Mount Okmok and Mount Kasatochi: In situ upper troposphere and lower stratosphere measurements of sulfate and organics over Europe, J. Geophys. Res., 115, D00L07, doi:10.1029/2009JD013628, 2010.

Schwarz, J. P., Gao, R. S., Fahey, D. W., Thomson, D. S., Watts, L. A., Wilson, J. C., Reeves, J. M., Darbeheshti, M., Baumgardner, D. G., Kok, G. L., Chung, S. H., Schulz, M., Hendricks, J., Lauer, A., Kärcher, B., Slowik, J. G., Rosenlof, K. H., Thompson, T. L., Langford, A. O., Loewenstein, M., and Aikin, K. C.: Single-particle measurements of midlatitude black carbon and light-scattering aerosols from the boundary layer to the lower stratosphere, J. Geophys. Res., 111, D16207, doi:10.1029/2006JD007076, 2006.

Sheridan, P. J. and Zoller, W. H.: Elemental Composition of Particulate Material Sampled from the Arctic Haze Aerosol, J. Atmos. Chem., 9, 363-381, doi:10.1007/BF00052843, 1989.

Sheridan, P. J., Brock, C. A., and Wilson, J. C.: Aerosol particles in the upper troposphere and lower stratosphere: Elemental composition and morphology of individual particles in northern midlatitudes, Geophys. Res. Lett., 21, 2587-2590, doi:10.1029/94GL01387, 1994.

Siddaway, J. M., and Petelina, S. V.: Transport and evolution of the 2009 Australian Black Saturday bushfire smoke in the lower stratosphere observed by OSIRIS and Odin, J. Geophys. Res., 116, D06203, doi:10.1029/2010JD015162, 2011.

Siebert, J., Timmis, C., Vaughan, G., and Fricke, K. H.: A strange cloud in the Arctic summer stratosphere 1998 above Esrange (68°N), Sweden, Ann. Geophys., 18, 505-509, doi:10.1007/s00585-000-0505-0, 2000.

Smekens, A., Godoi, R. H. M., Berghmans, P., and van Grieken, R.: Characterisation of soot emitted by domestic heating, aircraft and cars using diesel or biodiesel, J. Atmos. Chem., 52, 45–62, doi:10.1007/s10874-005-6903-7, 2005.

Solomon, S.: Stratospheric ozone depletion: A review of concepts and history, 37, 275-316, doi:10.1029/1999RG900008, 1999.

Song, J., Alam, M., and Boehman, A. L.: Characterization of diesel and biodiesel soot, Prepr. Pap.-Am. Chem. Soc., Div. Fuel Chem., 49, 767, 2004.

Stokes, D.J.: Principles and Practice of Variable Pressure/Environmental Scanning Electron Microscopy (VP-ESEM), John Wiley and Sons, Ltd, Publication, 221 pp., 2008.

Strand, L. D., Bowyer, J. M., Varsi, G., Laue, E. G., and Gauldin, R.: Characterization of Particulates in the Exhaust Plume of Large Solid-Propellant Rockets, J. Spacecraft Rockets, 18, 1981.

Strawa, A. W., Drdla, K., Ferry, G. V., Verma, S., Pueschel, P. F., Yasuda, M., Salawitch, R. J., Gao, R. S., Howard, S. D., Bui, P. T., Loewenstein, M., Elkins, J. W., Perkins, K., and Cohen, R.: Carbonaceous aerosol (soot) measured in the lower stratosphere during POLARIS and its role in stratospheric photochemistry, J. Geophys. Res., 104, 26753-26766, doi:10.1029/1999JD900453, 1999.

Testa Jr., J. P., Stephens, J. R., Berg, W. W., Cahill, T. A., Onaka, T., Nakada, Y., Arnold, J. R., Fong, N., and Sperry, P. D.: Collection of microparticles at high balloon altitudes in the stratosphere, Earth Planet. Sci. Lett., 98, 287-302, doi:10.1016/0012-821X(90)90031-R, 1990.

Thornberry, T., Froyd, K. D., Murphy, D. M., Thomson, D. S., Anderson, B. E., Thornhill, K. L., and Winstead, E. L.: Persistence of organic carbon in heated aerosol residuals measured during Tropical Composition Cloud and Climate Coupling (TC4), J. Geophys. Res., 115, D00J02, 2010.

Torvela, T., Tissari, J., Sippula, O., Kaivosoja, T., Leskinen, J., Virén, A., Lähde, A., and Jokiniemi, J.: Effect of wood combustion conditions on the morphology of freshly emitted fine particles, Atmos. Environ., 87, 65-76, doi:10.1016/j.atmosenv.2014.01.028, 2014.

Tumolva; L., Park, J.-Y., Kim, J.-S., Miller; A. L., Chow; J. C., Watson, J. G., Park, K.: Morphological and elemental classification of freshly emitted soot particles and atmospheric ultrafine particles using TEM/EDS, Aerosol Sci. Technol., 44, 202–215, doi:10.1080/02786820903518907, 2010.

Turco, R. P., Toon, O. B., Hamill, P., and Whitten, R. C.: Effects of Meteoric Debris on Stratospheric Aerosols and Gases, J. Geophys. Res., 86, 1113-1128, 1981.

Twohy, C. H., and Gandrud, B. W.: Electron microscope analysis of residual particles from aircraft contrails, Geophys. Res. Lett. 25, 1359-1362, doi:10.1029/97GL03162, 1998.

Vander Wal, R. L., Bryg, V.M., and Hays, M.D.: Fingerprinting soot (towards source identification): physical structure and chemical composition, J. Aerosol Sci., 41,108–117, doi:10.1016/j.jaerosci.2009.08.008, 2010.

Voigt, C., Schlager, H., Luo, B. P., Dörnbrack, A., Roiger, A., Stock, P., Curtius, J., Vössing, H., Borrmann, S., Davies, S., Konopka, P., Schiller, C., Shur, G., and Peter, T.: Nitric Acid Trihydrate (NAT) formation at low NAT supersaturation in Polar Stratospheric Clouds (PSCs), Atmos. Chem. Phys., 5, 1371-1380, 2005.

Weigel, R., Hermann, M., Curtius, J., Voigt, C., Walter, S., Böttger, T., Lepukhov, B., Belyaev, G., and Borrmann, S.: Experimental characterization of the COndensation PArticle counting System for high altitude aircraft-borne application, Atmos. Meas. Tech., 2, 243-258, doi:10.5194/amt-2-243-2009, 2009.

Weigel, R., Volk, C. M., Kandler, K., Hösen, E., Günther, G., Bogel, B., Grooß, J.-U., Khaykin, S., Bekyaev, G. V., and Borrmann, S.: Enhancements of the refractory submicron aerosol fraction in the Arctic polar vortex: feature or exception?, Atmos. Chem. Phys., 14, 12319-12342, doi:10.5194/acp-14-12319-2014, 2014.

Weinbruch, S., Benker, N., Kandler, K., Ebert, M., Ellingsen, D. G., Berlinger, B., and Thomassen, Y.: Morphology, chemical composition and nanostructure of single carbon-rich particles studied by transmission electron microscopy: source apportionment in workroom air of aluminium smelters, Anal. Bioanal. Chem., 408, 1151-1158, doi:10.1007/s00216-015-9217-x, 2016.

Wentzel, M., Gorzawski, H., Naumann, K.-H., Saathoff, H., and Weinbruch, S.: Transmission electron microscopical and aerosol dynamical characterization of soot aerosols, Aerosol Science, 34, 1347-1370, doi:10.1016/S0021-8502(03)00360-4, 2003.

Zolensky, M. E., and Mackinnon, I. D. R.: Accurate stratospheric particle size distributions from a flat plate collection surface, J. Geophys. Res., 90, 5801-5808, 1985.

Zolensky, M. E., McKay, D. S., and Kaczor, L. A.: A Tenfold Increase in the Abundance of Large Solid Particles in the Stratosphere, as Measured Over the Period 1976-1984, J. Geophys. Res., 94, 1047-1056, doi:10.1029/JD094iD01p01047, 1989.

Table 1: Sampling conditions

date (y/m/d/no)	sample	characteristics of flight*	PV at Θ [PVU]	altitude [km] pressure [hPa] potential temperature Θ [K] #	polar vortex
2000-01-20_07	A	PSC survey§	29.6	19.7/ 57/ 433	yes
2000-01-20_11	B	PSC survey§	27.7	19.4/ 60/ 431	yes
2000-01-23_18	C	vortex, sunrise	30.4	19.8/ 56/ 438	yes
2000-01-27_15	D	edge survey	30.3	19.9/ 56/ 448	no
2000-01-31_18	E	vortex survey	18.2	19.7/ 59/ 437	yes
2000-02-02_19	F	vortex survey	26.5	18.6/ 68/ 425	yes
2000-02-03_15	G	multiple level	32.0	17.4/ 83/ 400	yes
2000-02-26_12	H	vortex survey	24.7	19.1/ 62/ 430	yes
2000-02-26_14	I	vortex survey	31.3	17.3/ 64/ 431	yes
2000-03-05_19	J	vortex survey	26.6	19.2/ 64/ 424	yes
2000-03-11_19	K	vortex edge	26.2	18.7/ 66/ 430	yes

*according to Newman et al. (2002), #during sampling, § no particles out of PSCs were analyzed; PV= Potential Vorticity, PVU= Potential Vorticity Unit [10^{-6} K m^2 kg^{-1} s^{-1}]

Table 2: Absolute number of refractory particles within the four predefined particle groups.

Particle group	sample										
	A	**B**	**C**	**D**	**E**	**F**	**G**	**H**	**I**	**J**	**K**
C, O, Si	4	8	3	2	4	8	11	3	4	3	2
+ Cr, Fe, Ni	15	6	15	10	14	9	3	12	14	21	12
+ Cr, Fe	10	13	12	13	12	9	11	13	12	4	16
+ Fe	1	3	0	5	0	4	5	2	0	2	0

Table 3: Graphene sheet separation distance

Particle[#]	Separation distance [nm]		
	mean value	minimum - maximum	n
A-1	0.38	0.35 – 0.39	3
B-1	0.35	0.23 – 0.45	10
C-1	0.35	0.33 – 0.37	5
C-2	0.39	0.35 – 0.45	4
C-3	0.41	0.37 – 0.48	5
C-4	0.37	0.32 – 0.42	4
C-5	0.38	0.34 – 0.40	6
C-6	0.39	0.33 – 0.47	5
C-7	0.38	0.35 – 0.40	5
G-1	0.42	0.34 – 0.51	14
G-2	0.47	0.37 – 0.60	18
G-3	0.42	0.38 – 0.49	15
G-4	0.43	0.40 – 0.53	35
G-5	0.43	0.36 – 0.51	20
G-6	0.29	0.19 – 0.32	25
G-7	0.43	0.38 – 0.51	20
I-1	0.34	0.31 – 0.39	4
I-2	0.27	0.24 – 0.29	4
I-3	0.27	0.25 – 0.28	3
I-4	0.25	0.23 – 0.26	3
I-5	0.46	0.44 – 0.48	3
I-6	0.30	0.28 – 0.33	4
I-7	0.33	0.32 – 0.34	3

[#]sample-particle
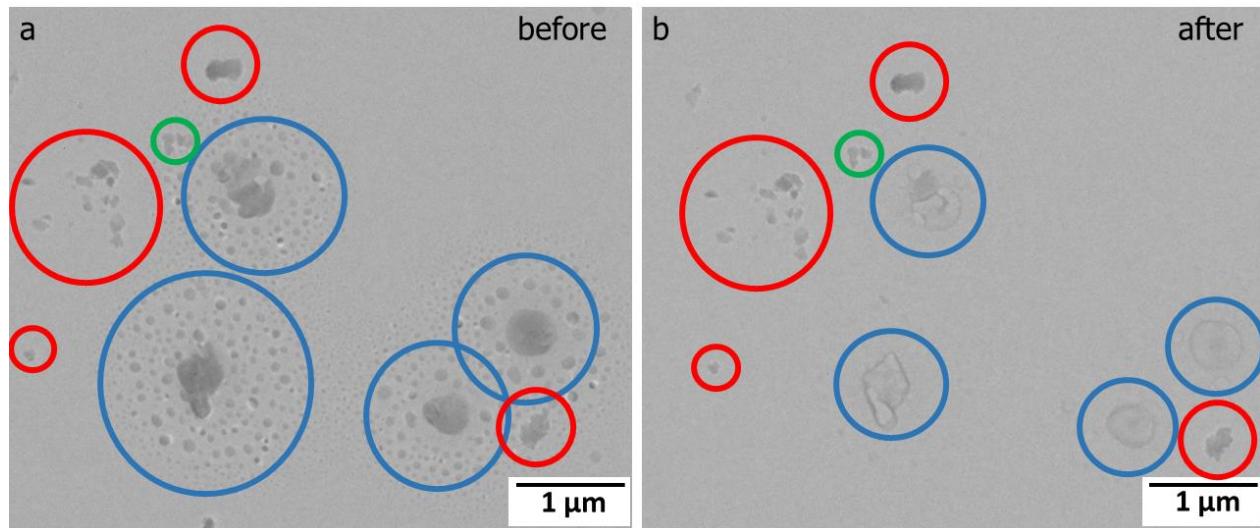
Figure 1: TEM bright field image of a typical sample (sample I; 17.3 km altitude), before (a) and after evaporation (b). Particles evaporating under electron bombardment are marked with blue circles. They consist of sulfates/hydrogen sulfates. Red circles indicate stable carbonaceous particles. Green circles show refractory carbonaceous particle internally mixed with volatile sulfates/hydrogen sulfates.
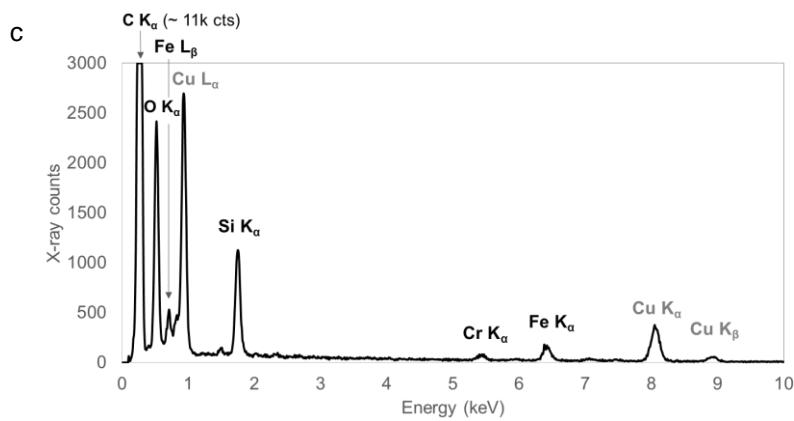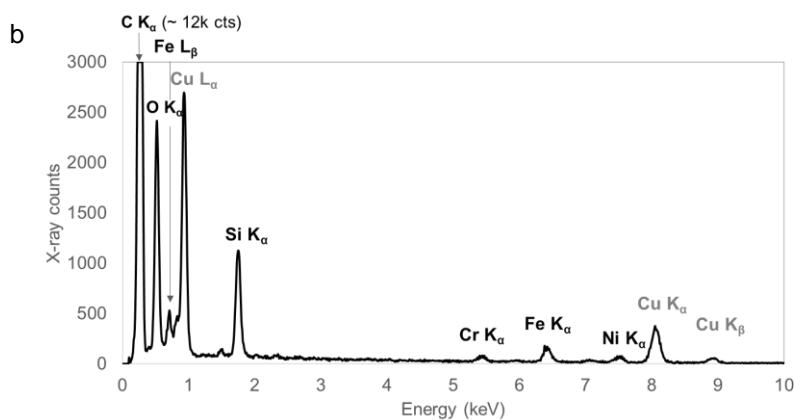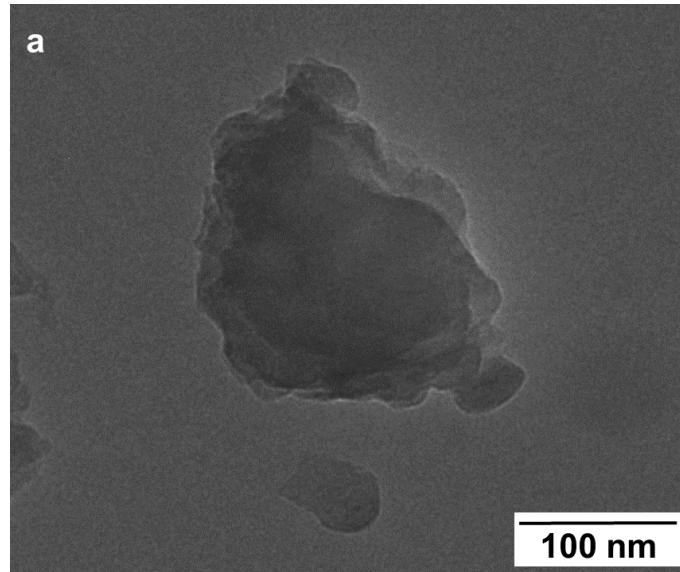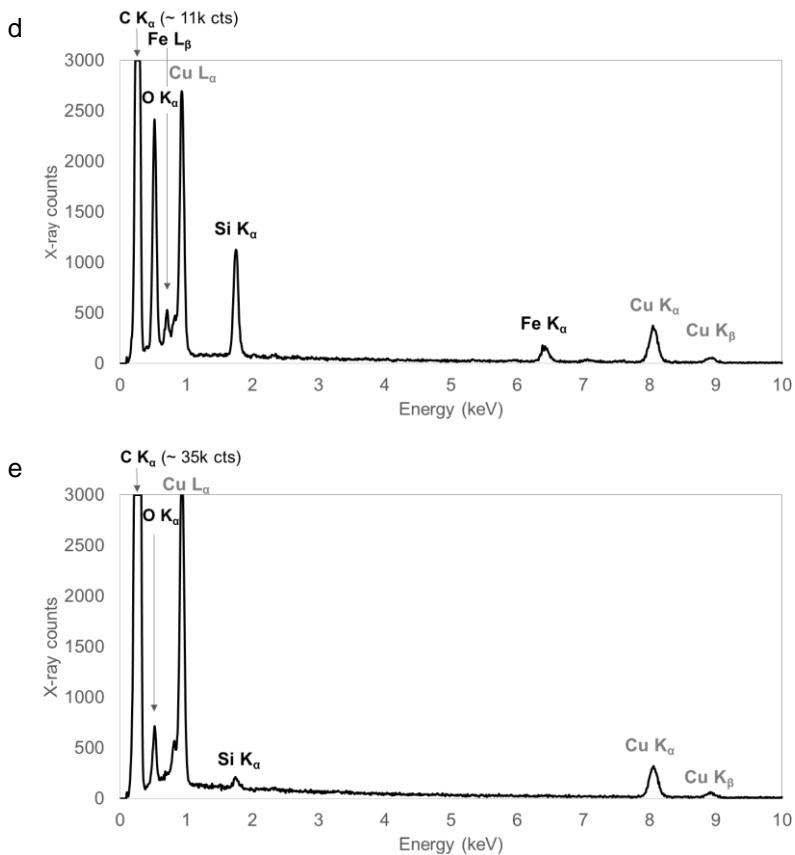
Figure 2: TEM bright field image (a) of a typical refractory carbonaceous particle from sample H (19.1 km altitude). The image is representative for all particles. The morphology is not depending on chemical composition, size, morphology or nanostructure. Energy-dispersive X-ray spectra of (b) a typical refractory carbonaceous particle with Fe, Cr and Ni, (c) Fe and Cr, (d) Fe and (e) without any other minor constitute. The particle predominantly consists of C and O. Minor amounts of Si are always present and may partly be an artifact of the substrate. Cu is an artifact from the TEM grid.
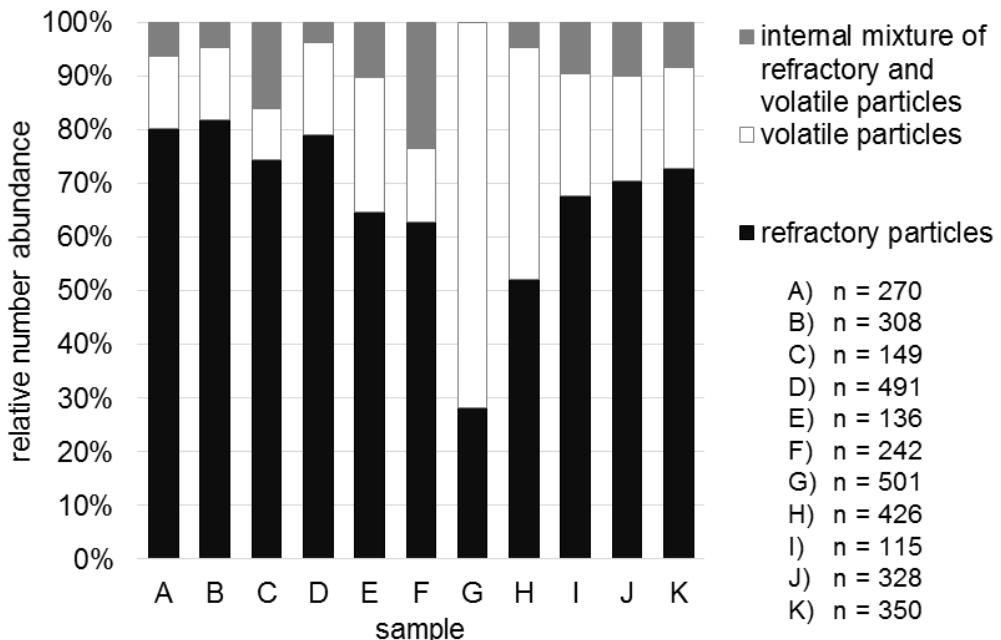
Figure 3: Relative number abundance of refractory carbonaceous and volatile particles as well as internal mixtures of both.
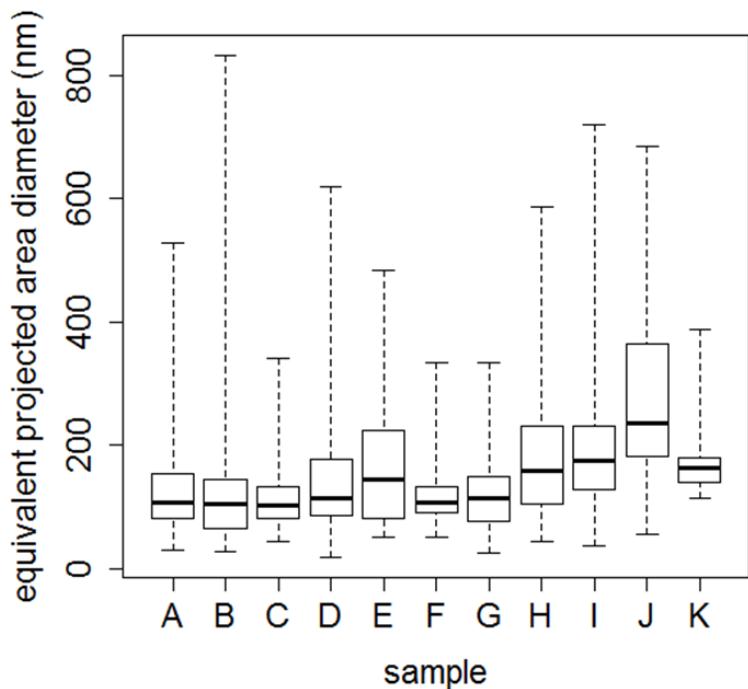
Figure 4: Boxplot of particle size (equivalent projected area diameter D_{pa}). Lower and upper quartiles appear as a box,
minimum and maximum values as whiskers.
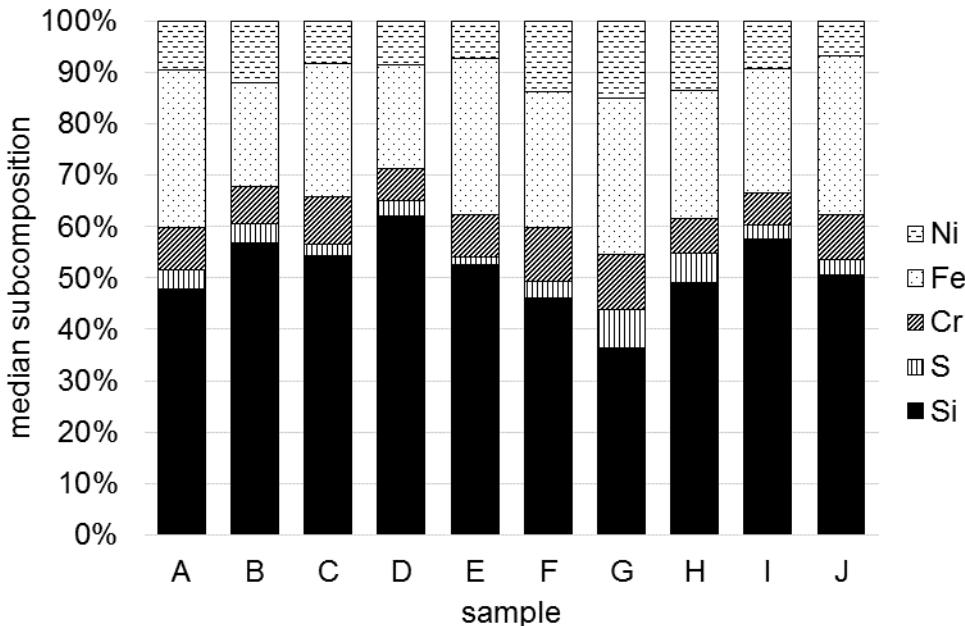
Figure 5: Median chemical subcomposition (atom %, without C and O) of refractory carbonaceous particles determined by SEM-EDX (30 particles per sample). Sample K was excluded from the figure due to a different substrate with higher Si content.
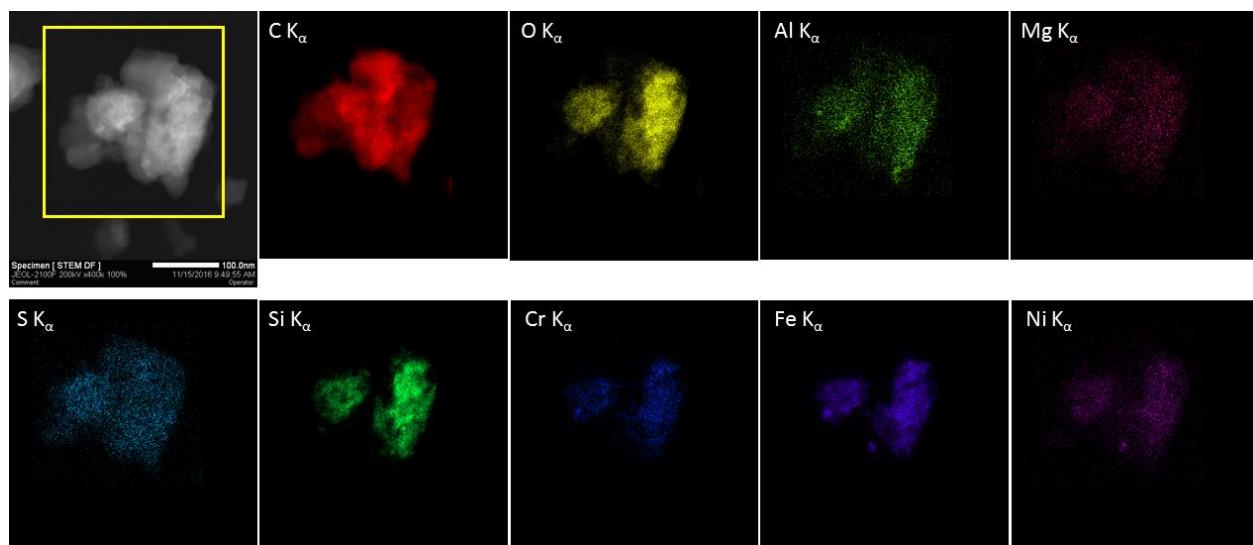
Figure 6: STEM image (upper left) and element distribution images of a refractory carbonaceous particle from sample C (19.8 km altitude).
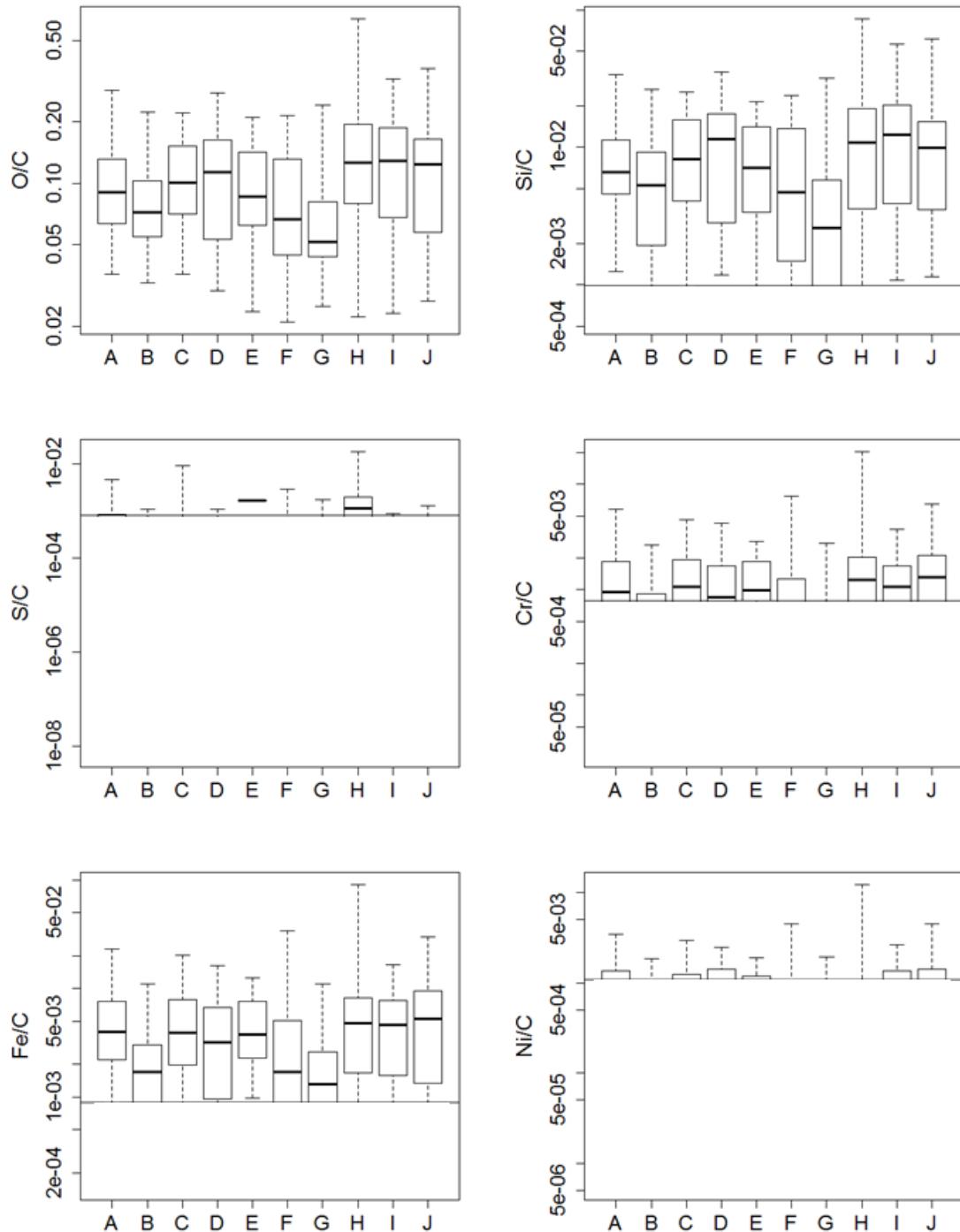
Figure 7: Censored boxplots of element ratios relative to C (atom %) determined by SEM-EDX (30 particles per sample). Sample K is not shown due to the different substrate used. Lower and upper quartiles appear as a box, minimum and maximum values as whiskers. Values below detection limit (horizontal line) are not shown.
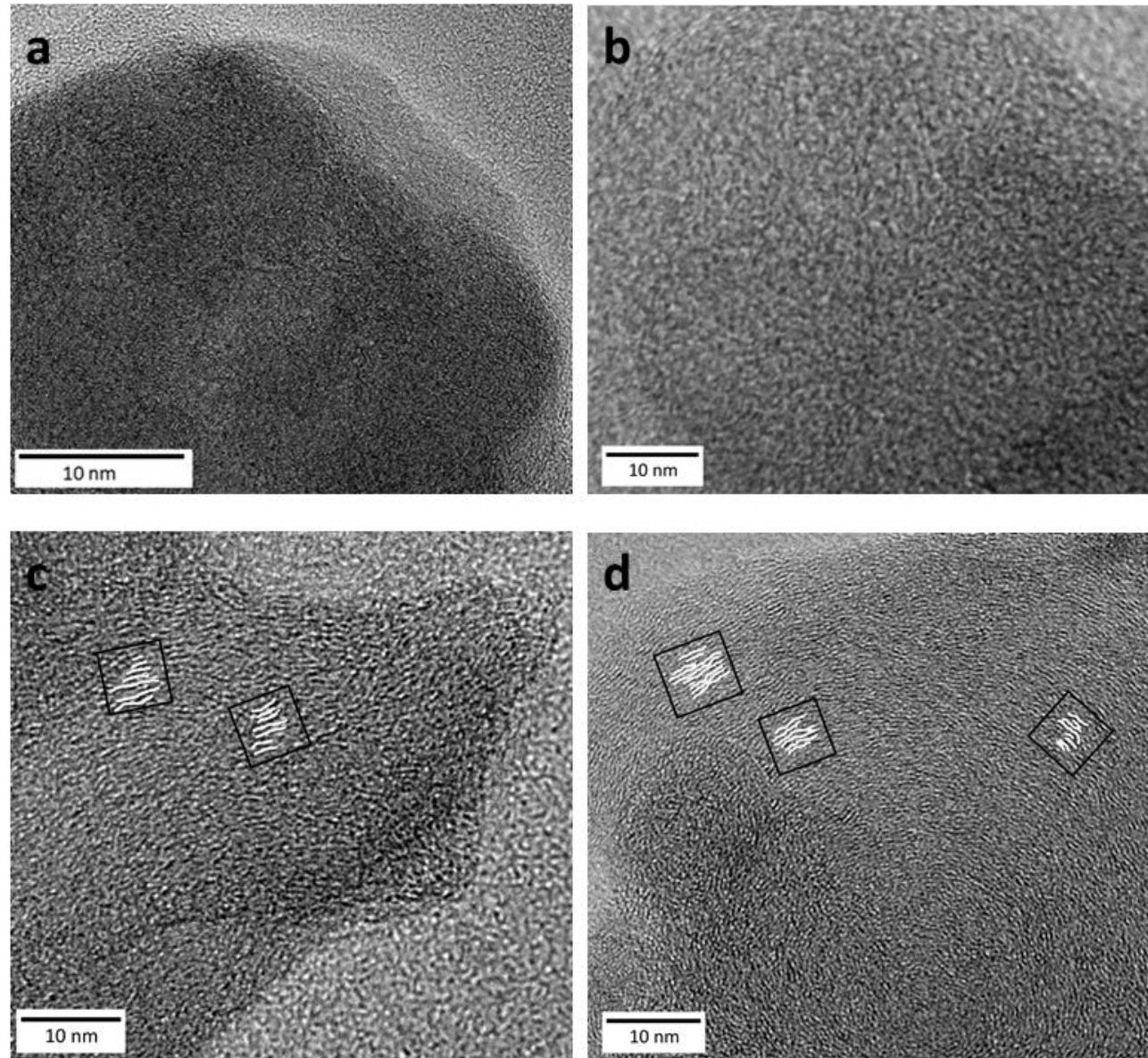
Figure 8: High resolution TEM image of individual refractory carbonaceous particles from sample G (17.4 km altitude): (a, b) completely amorphous particles, (c, d) particles showing small regions with ordering.
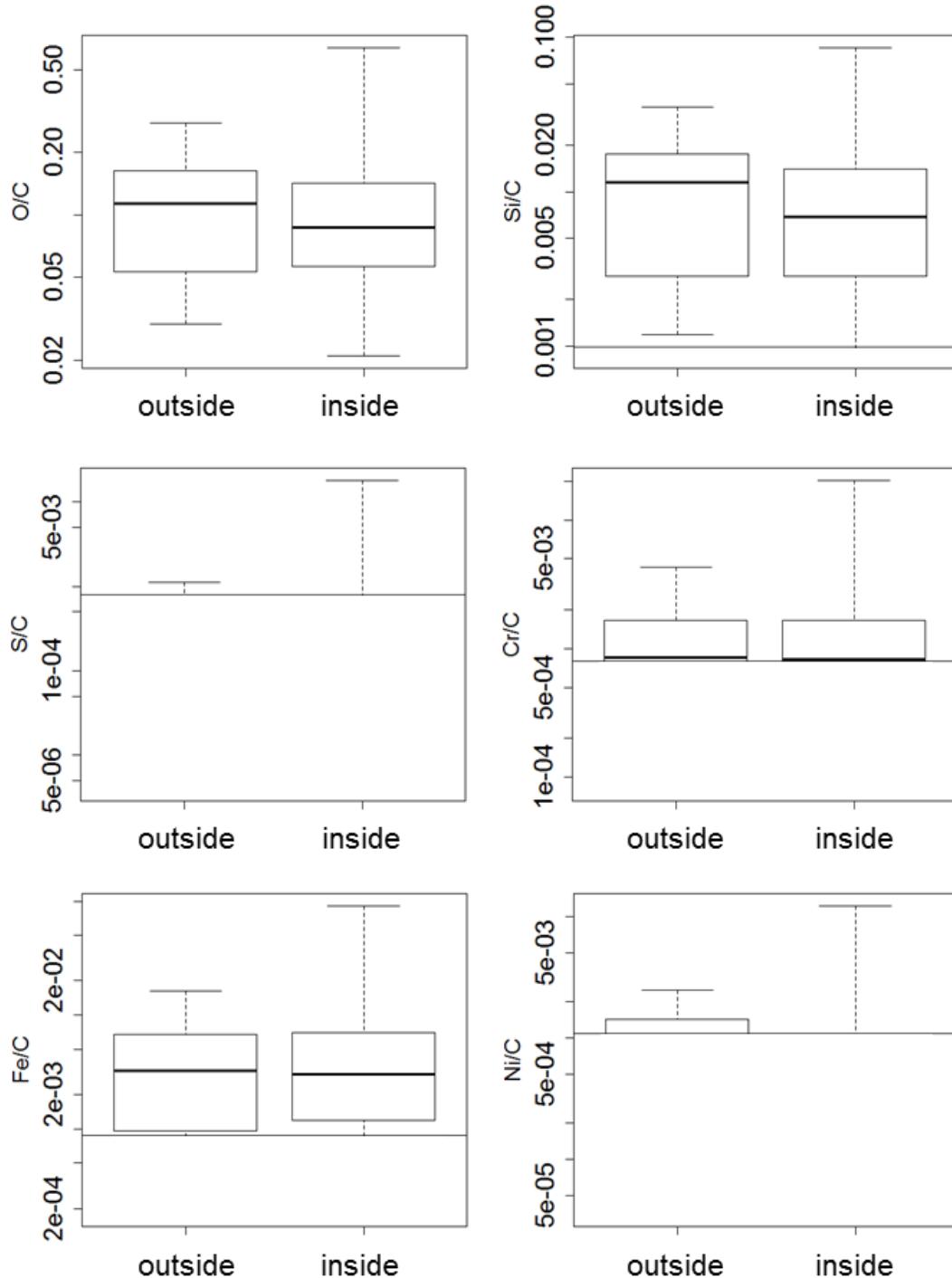
Figure 9: Censored boxplots of element ratios (atom %) relative to C, separately for outside and inside the polar vortex. Sample K was excluded from the analysis due to the different substrate used. Lower and upper quartiles appear as a box, minimum and maximum values as whiskers. Values below detection limit (horizontal line) are not shown.